Thesis for the degree of Licentiate of Engineering
in
Machine and Vehicle Systems

Safe distributed control allocation for articulated heavy vehicles

UMUR ERDİNÇ

Department of Mechanics and Maritime Sciences
CHALMERS UNIVERSITY OF TECHNOLOGY
Göteborg, Sweden 2024

Safe distributed control allocation for articulated heavy vehicles

UMUR ERDİNÇ

Thesis of Licentiate of Engineering 2024:03

Department of Mechanics and Maritime Sciences
Chalmers University of Technology
SE–412 96 Göteborg
Sweden
Telephone: +46 (0)31–772 1000

Chalmers Reproservice
Göteborg, Sweden 2024

Safe distributed control allocation for articulated heavy vehicles

Umur Erdinç
Department of Mechanics and Maritime Sciences
Chalmers University of Technology

Abstract

The electrification of trucks is now followed by the electrification of trailers. Additionally, the maximum allowed length of vehicle combinations has been increased in many countries to enhance efficiency. Electrification, increased variation, and complexity of multi-unit vehicle combinations have created the need for novel control allocation strategies. The traditional vehicle combinations are propelled only by the towing vehicle unit: trucks or tractors. Braking forces are distributed proportionally to the axle loads, which is commonly the safest approach. The modern combinations, on the other hand, may be propelled by multiple units. Regenerative braking may be performed by many electrified units, not necessarily in proportion to the axle loads. An optimal approach for the allocation of propulsion and brake forces into different vehicle units is power loss minimization. It may be more efficient to utilize only one of the vehicle units for propelling or regenerative braking from a power efficiency perspective. However, the most energy-efficient allocation may not be safe and can result in motion instability. For example, excessive regenerative braking with a tractor may lead to jackknifing. Hence, it is quite important to ensure the stability of the combination while allocating unit forces. This thesis introduces a safe operating envelope for vehicle combinations to ensure safe control allocation. Then the proposed safe operating envelope is tested using a real tractor-semitrailer combination, confirming its effectiveness in preventing yaw instabilities. In addition, some alternative methods in the force domain, and an alternative envelope in the tire slip domain are presented and evaluated with the real tests. The presented methods in this thesis showed promising performance in ensuring safety during the control allocation of unit forces at the combination level.

Keywords: Heavy vehicles, electric vehicles, control allocation, stability, jackknifing, trailer swing, power loss minimization

Acknowledgments

I wish to convey my heartfelt appreciation to my main supervisor, Assoc. Prof. Mats Jonasson, for his exceptional guidance, unwavering support, and fruitful discussions. I am also grateful to Prof. Bengt Jacobson for his invaluable advice and perceptive remarks. I extend special gratitude to my industrial supervisor, Adj. Prof. Leo Laine, for his unique perspective, inspiring motivation, and enthusiasm; and my co-supervisor, Prof. Jonas Fredriksson, for his excellent mentorship and his diligent review of my work. Thank you all for your immense contributions to my research journey.

I am deeply grateful to my industrial supervisor, Dr. Maliheh Sadeghi Kati, for her unwavering support and collaboration. It is hard to recall a day when she wasn't there to help me. Her invaluable help in reviewing all my papers is something I particularly appreciate. Thank you so much for everything.

I would like to express my sincere gratitude to my manager at Volvo, Simon Schoutissen, for his continuous encouragement and support. I have always been grateful for the significant contributions made by experts like Dr. Esteban Gelso, Dr. Leon Henderson, Christian Oscarsson, and numerous other colleagues at Volvo Group. The vehicle tests showcased in this thesis owe their success to the invaluable assistance and support from Dr. Fredrik Von Corswant of Chalmers REVERE, Tobias Johansson of VBG Group, and Tommi Saarikoski of Volvo Group. Our tireless efforts during the countless test days at Arjeplog were not in vain. My deepest thanks to everyone involved.

Special thanks to Sonja Laakso Gustafsson and all my colleagues at VEAS division at Chalmers for creating such a warm and delightful work atmosphere. It is an absolute pleasure to work alongside all of you. Every single moment shared with my roommate at VEAS, Sachin Janardhanan, was a joy. I am profoundly thankful for our effective teamwork and thought-provoking discussions.

Last but not least, I want to express my heartfelt gratitude to my mother, father, and sister. Their unwavering support throughout my life has been a beacon, guiding me through all my endeavors. Without them, I would not be where I am today. Finally, and most importantly, my best friend, constant companion, staunchest ally, source of joy, and my love, Direniş, this journey would have been unthinkable without your unwavering presence and support. I am incredibly thankful for your presence, your patience, and all the wonderful elements you have brought into my life!

This research has been made possible through financial aid from the Volvo Group and Vinnova, under the FFI program. I extend my sincere appreciation for this support.

Thesis

This thesis comprises a summary and is based on the following appended papers:

Paper A
U. Erdinc, M. Jonasson, M. S. Kati, B. Jacobson, J. Fredriksson, and L. Laine, ”Safe operating envelope based on a single-track model for yaw instability avoidance of articulated heavy vehicles,” *Vehicle System Dynamics*, Nov. 2023, doi: 10.1080/00423114.2023.2276767.

Paper B
U. Erdinc, M. Jonasson, M. S. Kati, B. Jacobson, J. Fredriksson, and L. Laine, ”Validation of high-fidelity simulation-based safe operating envelopes for articulated heavy vehicles using real test data,” *Vehicle System Dynamics*, Jan. 2024, doi: 10.1080/00423114.2023.2296595.

Paper C
U. Erdinc, M. Jonasson, M. S. Kati, B. Jacobson, J. Fredriksson, and L. Laine, ”Modelling of articulated heavy vehicles for computation of accurate safe operating envelope for yaw stability,” *17th International Symposium on Heavy Vehicle Transport & Technology (HVTT)*, Brisbane, Australia, Nov. 2023. Available: https://hvttforum.org/wp-content/uploads/2023/12/HVTT17_paper_3004_Erdinc.pdf

Paper D
U. Erdinc, M. Jonasson, M. S. Kati, L. Laine, B. Jacobson, and J. Fredriksson, ”Experimental validation of yaw stability control strategies for articulated vehicle combinations,” accepted for *35th IEEE Intelligent Vehicles Symposium*, Jeju, Korea, Jun. 2024.

Paper E
U. Erdinc, M. Jonasson, M. S. Kati, L. Laine, B. Jacobson, and J. Fredriksson, ”Yaw stability control of vehicles using a slip polytope validated with real tests,” accepted for *16th International Symposium on Advanced Vehicle Control*, Milan, Italy, Sep. 2024.

The following publication is relevant to the topic but not included in the thesis:

A. Hansson, E. Andersson, L. Laine, M. S. Kati, U. Erdinc, and M. Jonasson, ”Safe operating envelope for limiting actuation of electric trailer in tractor-semitrailer combination,” *2022 IEEE 25th Int. Conf. Intell. Transp. Syst. (ITSC)*, Macau, China, Oct. 2022, pp. 3886-3893, doi: 10.1109/ITSC55140.2022.9922094.

In addition, 19 patent applications in vehicle motion control have been filed directly as a result of this thesis.

Nomenclature

The nomenclature applies only to the thesis, but not to the appended papers.

Symbols

$a_{tractor}$	Tractor acceleration	m/s^2
$a_{trailer}$	Trailer acceleration	m/s^2
a_x	Longitudinal acceleration	m/s^2
a_y	Lateral acceleration	m/s^2
a_{xy}	Resultant acceleration	m/s^2
c_y	Normalized lateral acceleration	
$c_{tractor}$	Tractor driven axle friction utilization	
$c_{trailer}$	Trailer axle friction utilization	
g	Gravitational acceleration	m/s^2
F_{1rx}	Longitudinal force on tractor rear axle	N
F_{2x}	Longitudinal force on lumped trailer axle	N
F_y	Lateral force	N
F_{1rz}	Normal force on tractor rear axle	N
F_{2z}	Normal force on trailer axle	N
P_{loss}	Power loss	W
R	Wheel radius	m
S_x	Longitudinal slip	
V_x	Longitudinal velocity	
X	Global coordinate	m
Y	Global coordinate	m
α	Tire side-slip angle	$^\circ$
β	Body side-slip angle	$^\circ$
β_{1r}	Side-slip angle of tractor rear axle	$^\circ$
β_2	Side-slip angle of lumped trailer axle	$^\circ$
δ_{11}	Tractor steering angle	$^\circ$

μ	Road friction coefficient	
ω	Yaw rate	°/s
θ_{artic}	Articulation angle	°

Acronyms

ABS	Anti-lock braking system
AHV	Articulated heavy vehicle
ATC	AL-KO trailer control system
CAN	Controller area network
CCA	Combination control allocator
DI	Driver interpreter
EBS	Electronic braking system
ECU	Electronic control unit
EM	Electric motor
ESC	Electronic stability control
GPS	Global positioning system
ICE	Internal combustion engine
IMU	Inertial measurement unit
ME	Motion estimator
MLD	Maneuvering limitation diagram
MPC	Model predictive control
OEM	Original equipment manufacturer
PEM	Predictive energy management
RA	Rearward amplification
RSC	Roll stability control
SB	Service brake
SOE	Safe operating envelope
TEBS	Trailer electronic braking system
TSC	Trailer safety control
TSC	Trailer sway control
UCA	Unit control allocator
VTM	Volvo transport model

cap	Capability
des	Desired
lim	Limit
prop	Propulsion
ref	Reference
req	Request
stat	Status

Table of Contents

Chapter 1

Introduction

Heavy road vehicles play a crucial role in logistics and, therefore, are very important for fulfilling the demands of modern societies. Even though railway networks, marine, and aviation logistics have become more favorable in recent years, these modes of transportation typically cannot collect goods from their initial point of origin, nor can they deliver them to their ultimate destination. The initial and final stretches of transport, often spanning tens to hundreds of kilometers, largely rely on road vehicles. Hence, it's crucial now and in the future to ensure that transportation involving heavy vehicles is carried out as efficiently as possible. The crucial factor is not only economical efficiency but also reducing exhaust emissions. In light of these considerations, countries are increasingly permitting the use of longer heavy vehicle combinations. Additionally, the industry is witnessing a significant trend toward electrification, not only on heavy trucks but also on trailers. Given the growing complexity of heavy vehicle combinations, there is a pressing need for innovative approaches to vehicle motion control. The objective of this research is to devise control systems for multi-unit heavy vehicles that prioritize both safety and energy efficiency.

1.1 Background

In the European Union, the maximum permissible road train length is 18.75 meters, and the maximum weight is 40 tons with some exceptions [1]. The most popular vehicle combinations with these restrictions are tractor-semitrailer vehicle combinations, as shown in Fig. 1.1. In some countries of Europe, a maximum length of 25.25 meters and weight of 60 tons are permitted. For example, in Sweden, Nordic combinations consisting of a rigid truck, dolly, and semitrailer are quite popular. In 2023, Sweden, following in Finland's footsteps, permitted vehicle combinations that are 34.5 meters long and weigh up to 74 tons [2]. A typical long combination is an A-double combination, as shown in Fig. 1.1, with a tractor, dolly, and two semitrailers. Considering Nordic countries allowing for longer vehicle combinations with more units, it is expected that some other European countries will also follow this trend in the future [3].

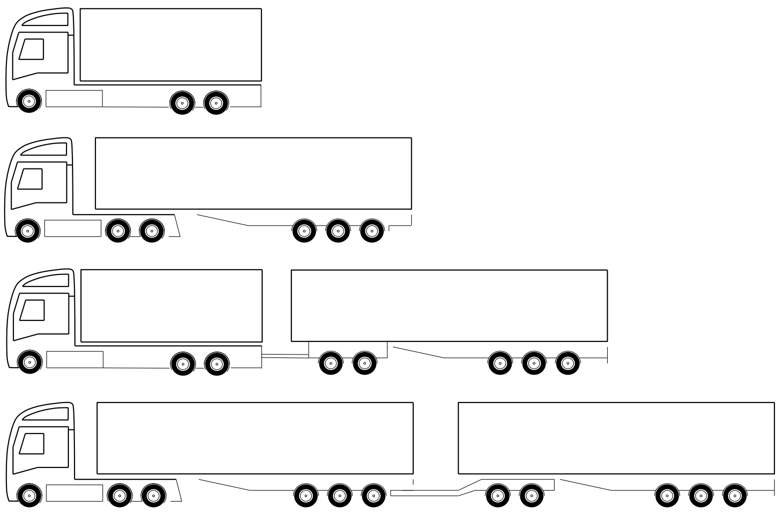

Figure 1.1: Different types of heavy vehicles (combinations): rigid truck (first), tractor-semitrailer combination (second), Nordic combination (third), A-double combination (fourth)

Electrification of vehicles affects not only the trucks and tractors but also trailing units such as semitrailers, and dollies. Electric trailers are already becoming commercially available products like ZF's [4], Trailer Dynamics's [5] and Einride's [6] e-trailers. These trailers have batteries and electric axles, thus can propel or brake with energy recuperation. They reduce fuel consumption and CO_2 emissions when towed by diesel trucks. In cases when they are towed by electrified trucks, they act as range extenders and traction boosters. There are also other examples like Schmitz Cargobull trailer [7], where the trailer can perform regenerative braking with a smaller electric motor, for example, to power a refrigeration system. In this case, propulsion with the electric motor is not possible.

Electrified units may have varying degrees of autonomy in their control systems. Some e-trailers may be controlled directly by the tractors. Some e-trailers may have internal controllers that receive less information from the tractors so that they can also be used combined with conventional ICE tractors. Some of the possible alternatives are listed below and summarized in Table 1.1. The types of E-trailers delineated in this thesis do not adhere to any established standard. Instead, they are classified in this manner to facilitate comprehension for the reader. For the sake of simplicity, an electric trailing unit is referred to as an e-trailer, but it can also be an e-dolly.

- **Type A**: E-trailer has electric motor(s) with a relatively small power capacity. This motor is used for only regenerative braking, and not for propulsion.

Table 1.1: E-trailer types. Sensors are given as examples but there may be deviations from the given list.

Type	**A**	**B**	**C**
Motor Power Capacity	low	high	high
Battery Capacity	low	high	high
Regenerative Braking	yes	yes	yes
Propulsion	no	yes	yes
IMU	yes	yes	yes
Articulation Angle Sensor	yes	yes	yes
Coupling Force Sensor	no	yes	no
Powering Auxiliaries	yes	yes	yes
Range Extender	no	yes	yes
Traction Booster	no	yes	yes
Startability Booster	no	yes	yes
Gradability Booster	no	yes	yes
Tractor Communication	minimal	moderate	extensive
Controller Computational Location	trailer	trailer	tractor

Regenerated energy is stored in a battery with relatively low capacity and used for the auxiliaries, such as powering a cooling system in a refrigerated semitrailer. Communication with the tractor is minimal, and a local controller in the e-trailer is coordinating the electric motor(s).

- **Type B**: E-trailer has electric motor(s) with higher power capacity. This motor is used for both regenerative braking and propulsion. Communication with the tractor is moderate, for example via ISO11992 interface, with brake request signals but lacking the acceleration request signals. A local controller in the e-trailer is coordinating the trailer propulsion, possibly with the help of data measured by, e.g., coupling force and articulation angle sensors. The e-trailer can act as a range extender, boosting the power, gradability, startability, and traction ability of the combination.

- **Type C**: Similar to type B in which the e-trailer has electric motor(s) with high power capacity for regenerative braking and propulsion, and acts as a range extender and power, gradability, startability, and traction booster. This type has the most extensive communication with the tractor, for example, via ISO11992 interface with additional signals such as acceleration request signals, or preferably high-speed automotive Ethernet. Control of the e-trailer can be performed by a controller located on the tractor, hence the controller has all the tractor signals in addition to the trailer states. There might be some sensor mounted on the e-trailer, such as an articulation angle sensor, but as both the tractor and e-trailer states are fully (or up to a great extent) known by the controller, there is no need for a coupling force sensor and the coupling forces can instead be estimated by the tractor and e-trailer forces.

Considering the varieties and technological potentials of the electrified vehicle combinations, novel motion control strategies are needed.

1.2 Motivation

Octopuses are the smartest invertebrate animals. These smart creatures can open jars, play with objects, and use tools. They surprise the scientists with not only their intelligence but also the allocation of this intelligence and decision-making ability to different parts of their bodies. Studies show that their arms can collect sensory information, and control their motions with partial autonomy without direct control of the central brain. Hence, each arm acts as if they have their own mini-brains [8]. In fact, around two-thirds of the neurons are located in the arms. When it comes to overall motion coordination and deciding the direction of travel, the central brain is in control. Levy et al. suggest that the central brain just decides which arm should move, but not how it moves [9]. Thanks to this distributed motion control with local "mini-brains", coordinated by a centralized main brain, the coordination of eight arms and allocation of motion into different arms become simpler and more efficient. Thus the central brain is not involved in very low-level decision-making, yet coordinates the overall motion.

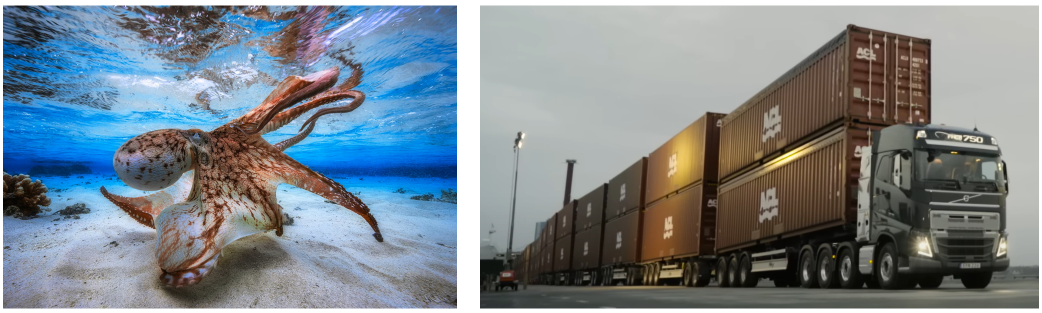

(a) An octopus with 8 arms collecting sensory information and controlling their own motions [10]

(b) A Volvo FH tractor towing 20 trailers and 750 tons [11]

Figure 1.2: An analogy of a multi-unit heavy vehicle combination and an octopus with multiple partially self-controlling legs

In Fig. 1.2, an octopus and a Volvo FH tractor towing 20 trailers are shown. It can be surprising for the readers to see an octopus in an engineering study and it may be hard to relate one to another. However, this analogy explains the core motivation of this study. The motivation is to bring a new perspective into multi-unit heavy vehicle control. The control architecture of such vehicle combinations should be similar to the control architecture of the octopuses. A centralized control allocator should allocate the control inputs of each vehicle unit, and each vehicle unit should perform lower-level actuator coordination. The upper-level controller should have access to the most important sensor and actuator information of each unit, without needing all the lower-level details. Leaving the more primitive control architecture of the traditional vehicles, and adopting this distributed control approach instead of a very centralized and complicated control strategy, it is possible to efficiently handle the complexities of the modern vehicle combinations with many electrified units. This study focuses on safe distributed control allocation for articulated heavy vehicles.

Allocating excessive propulsion or regenerative braking forces on certain units or axles aiming for the highest energy efficiency may result in motion instabilities such as jackknifing or trailer swing. Therefore it is important to allocate the forces not only considering the energy efficiency but also safety and stability. The safe allocation of the forces into various vehicle units should be performed by considering the envisioned distributed motion control architecture. Hence, a safe allocation should already be fulfilled when allocating unit forces in the higher-level controller. The focus of this study is this higher-level controller named as "combination control allocator". Particularly the safety aspect of the allocation is studied.

1.3 Research questions

The focus of the research in this thesis is the safety aspect of the control allocation. A safe operating envelope defining a set of operational limits and conditions of the vehicle states and actuator requests for a safe vehicle operation is particularly studied.

The following research questions are addressed in this thesis:

- How to define a safe operating envelope for multi-unit vehicle combinations so that a safe control allocation is performed in real-time without risking the stability of the vehicle?

- In which domains can the safe operating envelope be defined? Should it be defined in the force domain or slip domain?

- How should the control allocation functional architecture be for an efficient and distributed control?

1.4 Limitations

The scope of this study is limited to:

- instantaneous control allocation without involving any predictive control or predictive energy management,
- allocation of a total force request into different units at the combination level, without detailing the allocation at the unit level to each actuator,
- allocation of longitudinal forces, excluding any lateral motion quantity like the lateral forces, yaw moments, or steering angles,
- safe control allocation to maintain the stability of the combination, without focusing on the energy efficiency,
- maintaining the yaw stability of the combination, but not the roll stability,
- addressing divergent yaw instabilities like jackknifing and trailer swing, but not dynamic (oscillating) yaw instabilities like trailer sway,
- driving scenarios on the public road,
- either braking or propelling, but not propelling some axles and braking some other axles at the same time,
- control systems with knowledge of road friction coefficient and required vehicle states such as articulation angle, lateral acceleration, and yaw rates, obtained via sensors or a motion estimator.

1.5 Contributions

The contributions of this thesis to the literature are shown in Fig. 1.3. The main content and contributions are listed under each paper, together with (if applicable) the section or chapter that relates to the listed content.

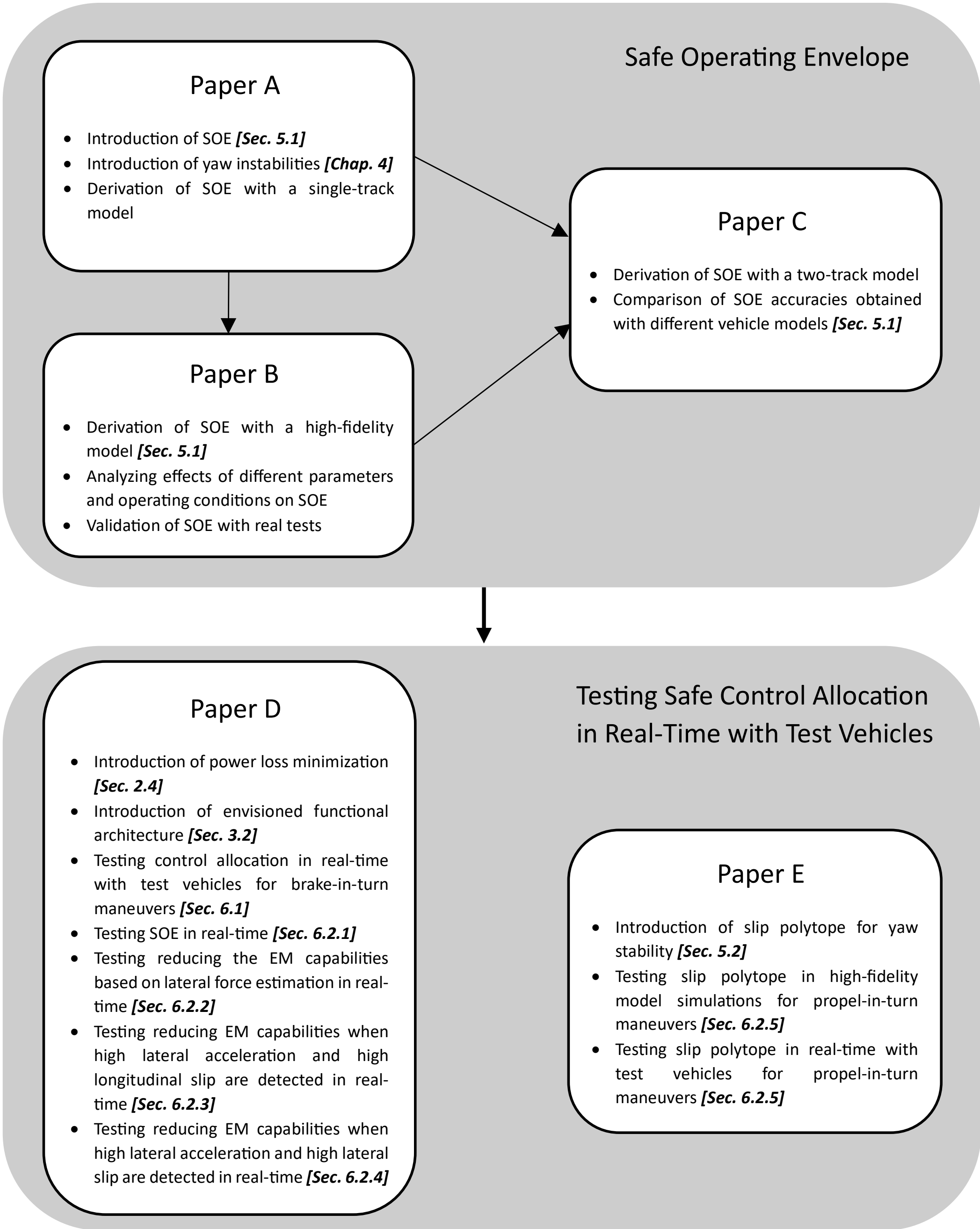

Figure 1.3: Content of the licentiate thesis

Chapter 2

Control allocation

Road vehicles historically had a simpler set of actuators to fulfill the motion request. Internal combustion engines were used to generate the longitudinal forces to accelerate the vehicle or to keep the speed. A steered front axle was used to steer the vehicle in the desired direction. Service brakes were used to slow down or stop the vehicle. With this trivial set of actuators, vehicle motion control was relatively simple. Directional control and propulsion control had trivial control strategies. The brake system, unlike the propulsion and steering systems, had some redundancy, meaning that there were multiple ways to obtain the same total brake force. Nevertheless, braking was performed with a fixed distribution among front and rear axle service brakes. In 1990s, electronic stability controllers were introduced, in which this redundancy was used to avoid instabilities, by means of using only a subset of service brakes. Modern heavy vehicles, on the other hand, have a much higher actuator redundancy, with the introduction of multiple actively steered axles, multiple electrified axles in each unit, and multiple electrified units. Hence, there are multiple ways to fulfill the motion requests due to this over-actuation. Unlike the traditional vehicles, now there is a more significant motivation to distribute the actuator requests in a more optimal way: energy efficiency within the multiple electric axles or multiple electrified units. Controlling an underdetermined vehicle system and solving for more vehicle inputs (actuator requests) than the number of the system of equations (degrees of freedom under control), also known as "control allocation", becomes significantly important when it comes to optimally distributing the actuator inputs while minimizing a cost function. This chapter first introduces the over-actuation of the heavy vehicles. Then reconfigurability and modularity of the controllers are discussed. Optimization-based control allocation is introduced. Finally, different ways of introducing safety constraints on the control allocator are explained.

2.1 Over-actuation

Traditional road vehicles have one actuator to control each of the longitudinal and lateral dynamics: an internal combustion engine and a steered axle. For braking, there are several service brakes, but apart from electronic stability controllers, the drivers or vehicle controllers merely benefit from this redundancy. Similar to traditional passenger vehicles, conventional Articulated Heavy Vehicles (AHV) also have no redundancy in propulsion and steering, as shown in Fig. 2.1.

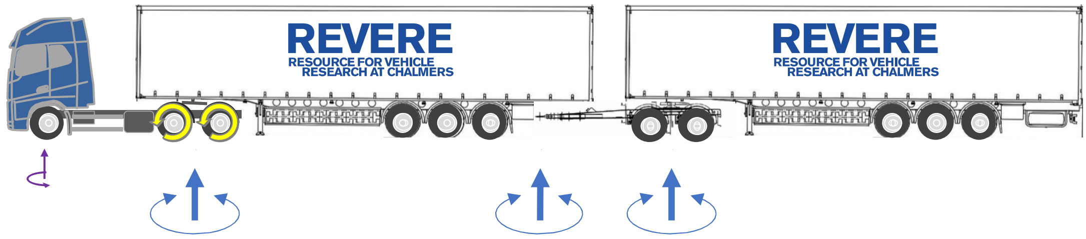

Figure 2.1: A conventional A-double combination vehicle. Purple arrows indicate steered axles, blue arrows indicate articulation points, and yellow arrows indicate diesel engine-propelled axles.

The electrification trend did not only affect the towing units of heavy vehicles, namely trucks or tractors, but also the trailing units, such as semitrailers and dollies. Thus, modern AHVs may have an extensive over-actuation in the electric propulsion systems, as shown in Fig. 2.2. In this example, all the axles of the tractor and dolly are electrified. Additionally, semitrailers also have electrified axles. Apart from the redundancy in the propulsion system, steering is also over-actuated thanks to the steered axles in all units.

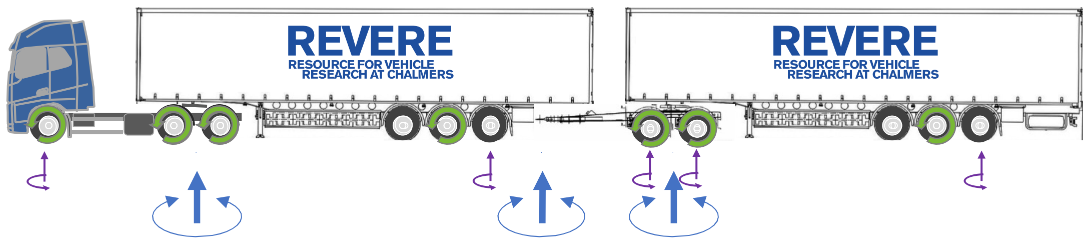

Figure 2.2: A modern A-double combination vehicle. Purple arrows indicate steered axles, blue arrows indicate articulation points, and green arrows indicate electric-propelled axles.

Electric motors, nowadays, are usually connected to the axles through gear trains and differentials, such as the case in Volvo FH trucks [12]. Furthermore, as hub-electric motors and individually propelled wheels are becoming popular, redundancy in the propulsion system can also generate yaw moment. Considering this extensive over-actuation in the modern AHVs, an optimal control allocation strategy becomes significantly important.

2.2 Reconfigurability

Considering the extensive variety in the number of units and unit types in the vehicle combination, control autonomy levels of the electrified trailing units, available sensor types and available signals for the control, reconfigurability has a significant importance in the control allocation of the combination vehicles. Laine classifies reconfigurability under the online and offline adaptivity [13].

- Offline reconfigurability means that the control system is easily configurable to adapt to various types and numbers of actuators, without changing the control law. Some examples are listed below.
  - The truck control system's parameters can be set at the factory enabling it to work with axle configurations of 4x2, 6x4, 8x4, and so on.
  - The combination control system's parameters can be set when the key is turned on via the information communicated by the trailing units, enabling it to work with a single conventional semitrailer or two e-trailers and a dolly as in an A-double combination, and so on.
- Online reconfigurability, on the other hand, is the ability of the controller to handle instantaneous operating conditions and limitations of the actuators and environment, and smooth arbitration for minimizing energy consumption and ensuring vehicle stability. Some examples are listed below.
  - The control system can adapt to changes in road friction, and other environmental parameters.
  - The control system can adapt if an actuator is faulty. The faulty actuator's capabilities are set as zero, and thus the control system prioritizes the usage of other actuators.
  - The control system can normally minimize energy consumption, but when instability is detected, it can rather prioritize safety over minimizing energy consumption.

Laine proposed a vehicle motion control system for a passenger car [13] that is offline and online reconfigurable. The aim of the studies presented in this licentiate thesis is to develop online and offline reconfigurable vehicle motion controllers for multi-unit vehicles that are easy to adapt for different vehicle and actuator combinations without changing the control law ensuring both vehicle stability and energy efficiency.

2.3 Algorithmic architectures

Vehicles historically have had distributed motion controllers: an engine controller for internal combustion engines, an electronic braking system (EBS) for controlling the service brakes, and a steering controller for the steered axle (for power-assisted steering or advanced driver-assistance systems like lane-keeping). Furthermore, each subsystem may have its layered control architecture to control the high-level dynamics or low-level actuator states. For example, a higher-level controller in EBS can distribute the brake forces into different axles, while a lower-level service brake controller can ensure that the requested brake force is fulfilled without causing a wheel lock.

Gäfvert [14] classified algorithmic partitioning with three structures as shown in Fig. 2.3.

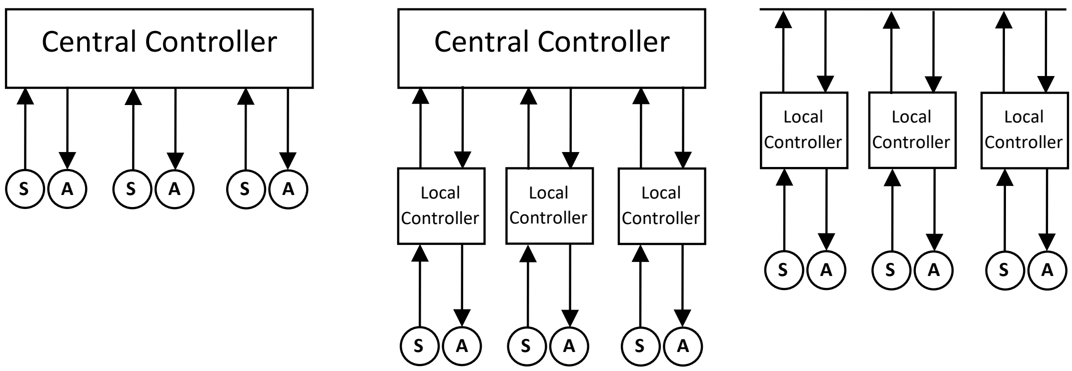

Figure 2.3: Algorithmic architectures: centralized (left), hierarchical (middle) and peer (right) structures. S denotes sensor, A denotes actuator. [14]

- **Centralized Structure**: All algorithmic blocks are merged into one central block, in which all the sensor data are received by this block and all actuators are actuated directly from this block. Although this architecture can outperform the distributed architectures [13], since all signals are simultaneously available for the controller, it lacks modularity, making it difficult to add new functionality or modify existing functions. A centralized controller is the least reconfigurable structure.

- **Hierarchical Structure:** An upper-level central controller coordinates different local controllers. Each local controller has access to actuators and sensor data. This structure has modularity and distributed control, yet with coordination done by the central controller. A hierarchical architecture has high reconfigurability.

- **Peer Structure:** Algorithms are partitioned with no explicit hierarchy. There is no upper-level controller that coordinates different local controllers but the local nodes can share information in between. This is the most modular structure with many distributed controllers but lacking the coordination done by the central controller, hence conflicts between different local nodes may happen.

Traditional vehicles with distributed motion controllers fall into the peer structure. The internal combustion engine is controlled with a local engine controller, the brakes are controlled with another local controller (typically an EBS system), and advanced steering functions are controlled with another local steering controller. With the electrification trend, brake blending became an important factor in minimizing energy consumption. Hence, it is important to coordinate the service braking with regenerative braking performed by the electric motors. The brake blending function in modern vehicles falls into the hierarchical structure since the total brake force is computed at an upper-level controller and then distributed into the electric propulsion and service brake systems. Laine [13] proposed a hierarchical structure to coordinate these systems for a passenger car. Driver interpreter, path controller, and control allocator are 3 layers of the vehicle motion control system that are located at the upper hierarchical level. Local controllers of each actuator system are located at the lower hierarchical level. Hence, the upper-level vehicle motion controller coordinates the lower-level controller nodes for service brakes, internal combustion engine, and (if autonomously steered) steering system.

Ghandriz [17] adapted the hierarchical structure for predictive energy management for hybrid electric heavy vehicle combinations. In his work, the tractor is driven by an ICE, and the dolly is electrified in an A-double combination. He adapted a first control layer for velocity, battery energy, and gear planning, a second control layer for vehicle velocity tracking, and a third control layer for actuator control.

Considering only the control allocation, and ignoring the other controllers such as path followers, reference force generators, and predictive energy management, the algorithmic architectures shown in Fig. 2.3 can be depicted for the multi-unit control allocation problem as in Fig. 2.4. Ghandriz's algorithmic architecture presented in [17] is hierarchical considering the overall control scheme, but it can be either centralized in the sense that a single centralized control allocator allocates the individual actuator requests of each different vehicle unit, such as tractor, dolly, and semitrailers, or it can generate reference signals for the unit control allocators to follow in a hierarchical structure.

A centralized control allocator can outperform (in terms of safety and energy efficiency) the distributed control allocators due to its access to all control signals

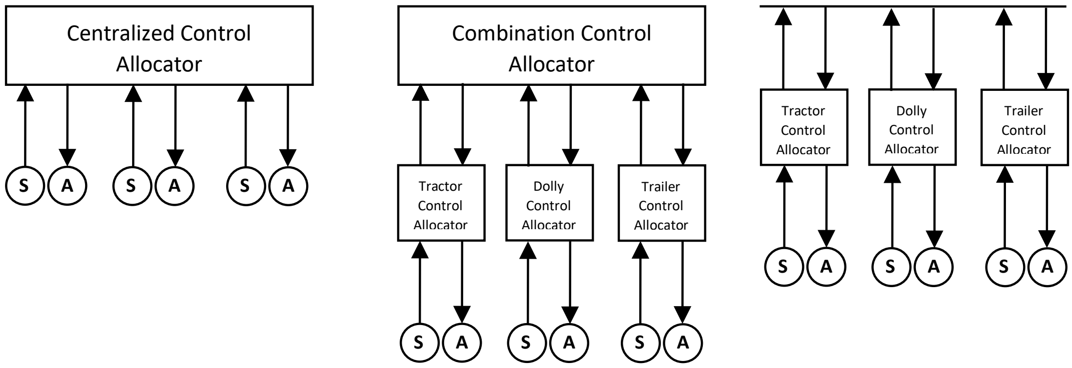

Figure 2.4: Control allocation architectures for multi-unit vehicles: centralized (left), hierarchical (middle) and peer (right) structures. S denotes sensor, and A denotes actuator.

and sensor data. However, in the scope of the studies presented in this licentiate thesis, a hierarchical control allocation, with a combination control allocator and a local control allocator for each unit is aimed. Particularly the combination control allocator is studied. The hierarchical architecture brings the advantage of high reconfigurability for different types and numbers of trailing units. Furthermore, thanks to the distributed control architecture, the local controllers can be run in different electronic control units (ECU) which may be located in the same or different vehicle units. Peer structure in the control allocation for multi-unit vehicles would be the case with a conventional ICE tractor and e-trailer (hybrid combination). In this case, e-trailers may have local control allocators without the need for an upper-level combination control allocator or an extensive set of signals from the tractor. Nevertheless, a hierarchical control allocation strategy may be reconfigured to be used with such e-trailers, and still supports the ability to coordinate the local control allocators of suitable e-trailers.

2.4 Optimization-based control allocation

Solving a control problem for an over-actuated dynamical system and distributing the control requests into several actuators to fulfill a set of reference signals is called "control allocation". For a reference set of control signals (such as total longitudinal and lateral force, and yaw moment on the vehicle), $\mathbf{v}$, also named as "virtual control input vector", and for a linear control problem that outputs the actuator requests (such as electric motor and service brake torques and steering angle), $\mathbf{u}$, the problem can be formulated as:

$$\mathbf{v} = \mathbf{B}\mathbf{u} \tag{2.1}$$

where $\mathbf{B}$ is called the "control effectiveness matrix" and $\mathbf{v} \in \mathbb{R}^{k\times1}$, $\mathbf{u} \in \mathbb{R}^{m\times1}$, $\mathbf{B} \in \mathbb{R}^{k\times m}$. If $k = m$, which means the number of virtual control inputs and the actuator requests are equal (hence the system is fully actuated), and $\mathbf{B}$ is invertible, then (2.1) can be solved for the solution $\mathbf{u*}$ as:

$$\mathbf{u*} = \mathbf{B}^{-1}\mathbf{v} \tag{2.2}$$

In this trivial case, $\mathbf{B}$ is a square matrix, and the system has no redundancy. In the case of over-actuation with $k < m$ for an underdetermined system, matrix $\mathbf{B}$ is not square and not invertible. Hence, there is a need for a more advanced method instead of (2.2). There are multiple options for control allocation, such as pseudo-inverse, direct allocation, daisy-chaining, and optimization-based methods [16]. Here, optimization-based methods will be elaborated.

Solving the control allocation problem with optimization brings the benefit of adding multiple objectives to the problem, apart from fulfilling the virtual control input signals. Härkegård [18] and Laine [13] solved the control allocation problem for the flight control and vehicle control, respectively, with the following formulation:

$$\mathbf{u*} = \arg\min_{\underline{\mathbf{u}}\leq\mathbf{u}\leq\bar{\mathbf{u}}} \|\mathbf{W_u}(\mathbf{u} - \mathbf{u}_{\text{des}})\|_2 + \gamma\,\|\mathbf{W_v}(\mathbf{Bu} - \mathbf{v})\|_2 \tag{2.3}$$

The first term $\|\mathbf{W_u}(\mathbf{u} - \mathbf{u}_{\text{des}})\|_2$ is for tracking the reference desired control inputs, $\mathbf{u}_{\text{des}}$. Desired control inputs can be sent from, e.g., the energy management and steering controllers. Even if there is no reference signal sent from such controllers, this term penalizes the usage of any actuators, that can, e.g., be useful to avoid actuator fights, such as front axle propelling and rear axle braking. $\mathbf{W_u}$ is the weighting matrix for setting the weights of each reference input tracking term. The second term $\|\mathbf{W_v}(\mathbf{Bu} - \mathbf{v})\|_2$ is for fulfilling the desired motion of vehicle. $\mathbf{W_v}$ is the weighting matrix for setting the weight of each virtual control input term. γ is another weighting factor for setting the prioritization of the second term over the first term. $\underline{\mathbf{u}}$ and $\bar{\mathbf{u}}$ are the minimum and maximum actuator capabilities, respectively. The formulation is solved with norm-2, hence it becomes a quadratic problem. Alternatively, the second term can be written as an equality constraint and only the first term can be optimized.

For vehicles with multiple electric motors, a power loss minimization problem can be solved by distributing the motor torques in an energy-efficient way [19], [20]:

$$\begin{aligned} &\mathbf{u*} = \arg\min_{\underline{\mathbf{u}}\leq\mathbf{u}\leq\bar{\mathbf{u}}} P_{loss}(\mathbf{u}) \\ &\text{s.t. } \mathbf{v} = \mathbf{Bu} \end{aligned} \tag{2.4}$$

In this formulation, instead of reference input tracking term, $\|\mathbf{W_u}(\mathbf{u} - \mathbf{u}_{\text{des}})\|_2$, the total power loss (due to electric motor losses, inverter losses, driveline, and battery losses), $P_{loss}(\mathbf{u})$, is minimized. These losses are usually approximated as a quadratic power loss function for a given motor speed, hence the formulation becomes a quadratic problem that is easier to solve. Fulfilling the reference virtual control inputs, $\mathbf{v}$, is done via the equality constraint.

In the literature, control allocation is also done in combination with predictive energy management, considering road profile for 5 to 20 km horizon [17]. However, in the studies presented in this licentiate thesis, only instantaneous control allocation is considered.

2.5 Stability constraints

While allocating the actuator inputs, it is important to maintain the stability. Allocating too much force on the driven axle of the tractor may cause jackknifing, especially on slippery roads with low friction and sharper curves. Likewise, allocating large forces on the trailer axles may result in trailer swing. Both incidents are significantly risky and may lead to fatal accidents. Hence, it is important to avoid the risky allocation of forces.

A set of inequality constraints can be added to the control allocation problem given in (2.4) as follows:

$$\mathbf{Au} \leq \mathbf{b} \tag{2.5}$$

where matrix $\mathbf{A}$ and vector $\mathbf{b}$ represents the inequality conditions imposed on the allocated actuator requests $\mathbf{u}$. Matrix $\mathbf{A}$ and vector $\mathbf{b}$ can be functions of some of the vehicle states, such as lateral acceleration. Inequality constraints formulated in (2.5) can be used, for example, to avoid too much tractor braking if the trailer is not braking, and vice versa, at high lateral accelerations. This method will be elaborated in Chapter 5.

If the actuator force constraints are straight-forward and do not relate to each other, they can simply be implemented by using upper and lower bounds for $\mathbf{u}$: $\underline{\mathbf{u}}$ and $\bar{\mathbf{u}}$. As an example, longitudinal forces applied by the service brakes and electric motors can be limited considering the lateral force estimations and a friction circle as explained in Section 6.2.2.

Chapter 3

Envisioned functional architecture and interface

Communication between different units of the heavy vehicle combinations, historically, is performed via ISO 11992 CAN network. The signal database of this network is quite limited since traditional trailers have no propulsion system, hence this communication mostly serves for braking the trailers. Furthermore, the control systems in the trailers are very limited, mostly with Trailer Electronic Brake System (TEBS) and air suspension controllers. Electrification of modern heavy vehicle combinations requires novel standardized interfaces and functional architecture. In this chapter, first, the current functional architecture and interface in the combination vehicles are explained, and then the envisioned architecture and interface are introduced.

3.1 Current functional architecture and interface

Antilock Braking System (ABS) is mandatory for trailing units in European heavy vehicle combinations. ABS is typically integrated into Electronic Braking Systems (EBS) together with electronic brake force distribution and Roll Stability Control (RSC). Furthermore, heavy trailers are mostly equipped with air suspension systems. Apart from these systems, trailers are not typically equipped with other functions or actuators. Trailers' functions and the number of Electronic Control Units (ECU) are therefore very limited, compared to towing vehicles like rigid trucks or tractors.

A simplified form of the functional architecture of a Nordic combination consisting of a truck, dolly, and semitrailer is shown in Fig. 3.1. Although the detailed computational nodes and interfaces are simplified and some actuators and control systems (such as air suspension systems) are not shown for the sake of simplicity, the main control systems and actuators are illustrated. Sensors are depicted in orange, and actuators are shown in blue.

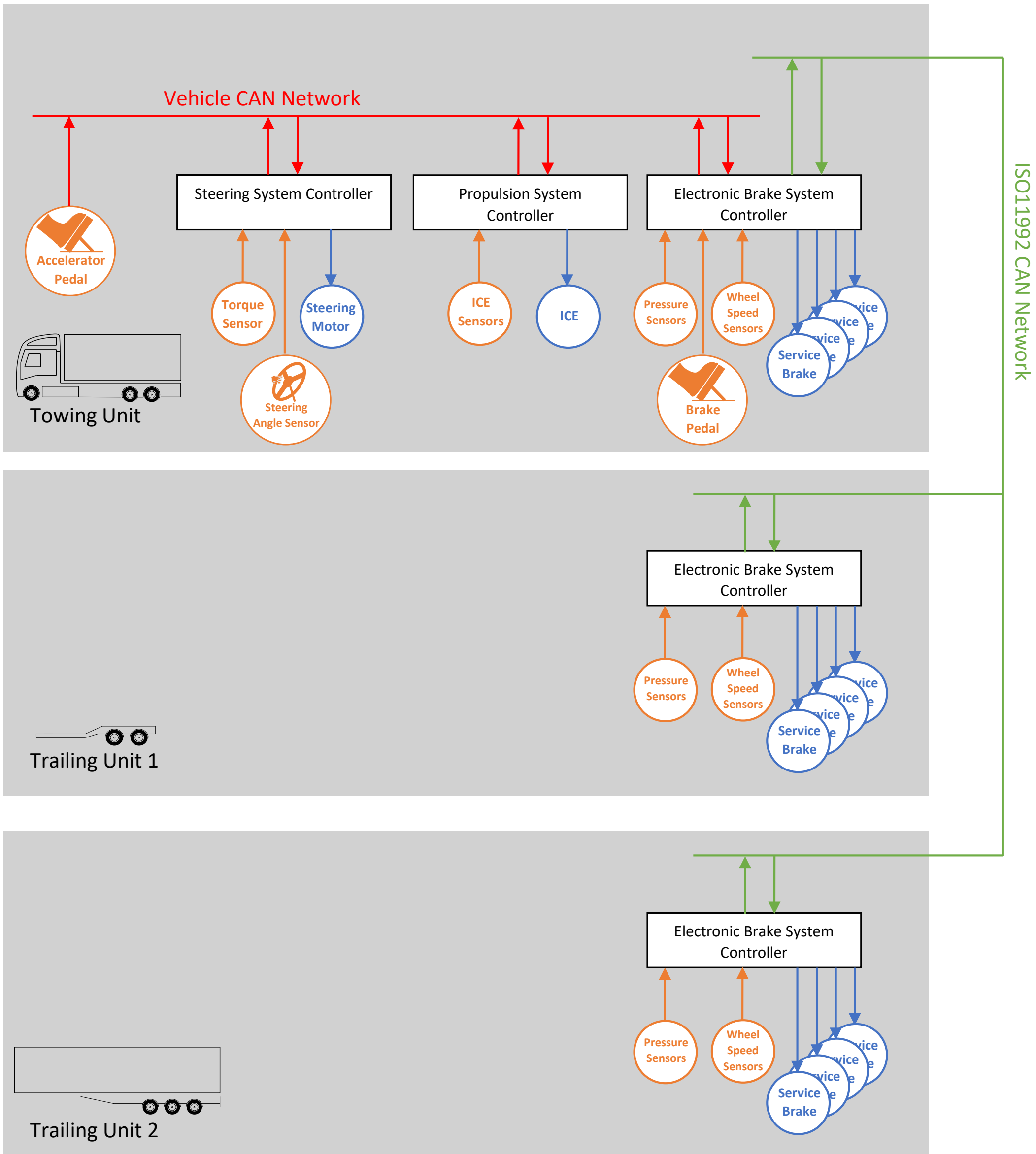

Figure 3.1: Functional architecture of traditional European heavy vehicle combinations

The steering controller, in the case of an advanced steering system that, for example, has lane-keeping assist (hence a steering motor for generating torque), has access to the steering wheel angle, and torque measurements on the steering column. By using these signals, the steering controller controls the steering motor.

The propulsion system controller can access various internal combustion engine (ICE) sensors and control the ICE according to the accelerator pedal position. The accelerator pedal signal is not only communicated to the propulsion system, but it is also available to many of the other controllers. Hence in the figure, it is shown as connected to the vehicle CAN network.

The electronic braking system is typically not developed by the automotive Original Equipment Manufacturers (OEM) but is outsourced, together with the service brake actuators and sensors. Heavy vehicles are equipped with pneumatic brakes. Among others, pressure sensor and wheel speed sensor measurements are communicated to the EBS controller. Furthermore, the brake pedal sensor is usually directly read by the EBS. Then EBS controls the service brakes accordingly. Brake forces are distributed considering the axle loads.

Trailer EBS is also mostly similar to truck EBS, but as it has no information regarding the brake pedal position, truck EBS is communicating an overall retardation request to the trailer EBS via ISO 11992 standardized CAN network [21]. A small amount of modification on the retardation request can be done by the tractor EBS as a part of coupling force control, but this amount is very limited in magnitude. The only exception to this is during stability control events, the truck can take more control of the combination and request braking from the trailers that may be different from the retardation target for the truck.

ISO 11992 CAN network is defined by the corresponding ISO standard and has limited content. For example, it has no information regarding the accelerator pedal position or acceleration target of the truck. However, for conventional trailers, this extensive set of signals is not needed since the trailers are not propelled.

From Fig. 3.1, it is evident that the algorithmic architectures of the vehicle combination systems are mostly peer structures, as explained in Section 2.3. Steering, propulsion, and braking systems control the motion actuators without an upper-level coordinator, although they communicate with each other via a vehicle CAN network. Furthermore, the overall combination control is also similar to peer structure as each unit's EBS is controlling the service brakes of the corresponding unit, with no upper-level coordinator, yet they communicate with each other via ISO 11992 CAN network.

Integrating electrified powertrains and advanced steering systems into the trailing units requires a more advanced functional architecture and interface. In the following sections, the envisioned architecture and interface are elaborated.

3.2 Envisioned functional architecture and interface

Envisioned functional architecture for a Nordic combination (as an example) that consists of an electric truck, actively steered dolly, and electric semitrailer is shown in Fig. 3.2.

The accelerator pedal, brake pedal, and steering wheel inputs are received by a Driver Interpreter (DI). The DI then communicates the acceleration request (positive or negative) to the Combination Control Allocator (CCA). The CCA, in turn, sends back status and capability signals of acceleration and curvature to the DI. The Motion Estimator (ME) reads GPS, IMU, wheel speed sensors, and others; communicates the estimated vehicle states, such as unit speeds, yaw rates, side-slip angles, articulation angles, road friction, unit masses, total driven and non-driven axle loads of the units, and so on.

The CCA distributes the total Electric Motor (EM) and Service Brake (SB) forces among different units of the combination, with lower-level actuator allocation managed by Unit Control Allocators (UCA). For the CCA to allocate the unit-wise forces, the UCAs send the status and capability signals back to the CCA. An important signal worth mentioning is the unit-wise lumped electric motor power loss maps. The lumped maps provide an overall power loss representation of the unit in a single map even though there may be several EMs in a unit. It also includes losses in the gear trains, inverters, and batteries. For a quadratic approximation, the power loss corresponding to the instantaneous operating speed of the EMs consists of three parameters (for quadratic, linear, and constant terms), hence all these three parameters are communicated. In the case of EMs that are possible to turn off or de-clutch, the UCA may send several alternative lumped power loss maps to the CCA, with and without some EMs turned off, and the CCA can allocate the unit forces considering the most optimal case in terms of power efficiency.

The UCA of each unit allocates the actuator forces to EMs and SBs. The EBS controller and propulsion system controller are still present in Fig. 3.2, but their role involve lower-level actuator control, such as controlling the voltage and current for the EMs and pneumatic pressures for the SBs. Hence, the EBS supports individual external braking via an upper-level controller such as the UCA. The UCA also performs power loss minimization in the case of a unit with multiple EMs, but at the unit level.

Communication between the CCA and UCAs can be performed via an automotive Ethernet connection that supports much faster speeds, hence many more signals can be sent over the communication line with higher resolutions and higher frequency. However, the limited example set of signals shown in Table 3.1 can

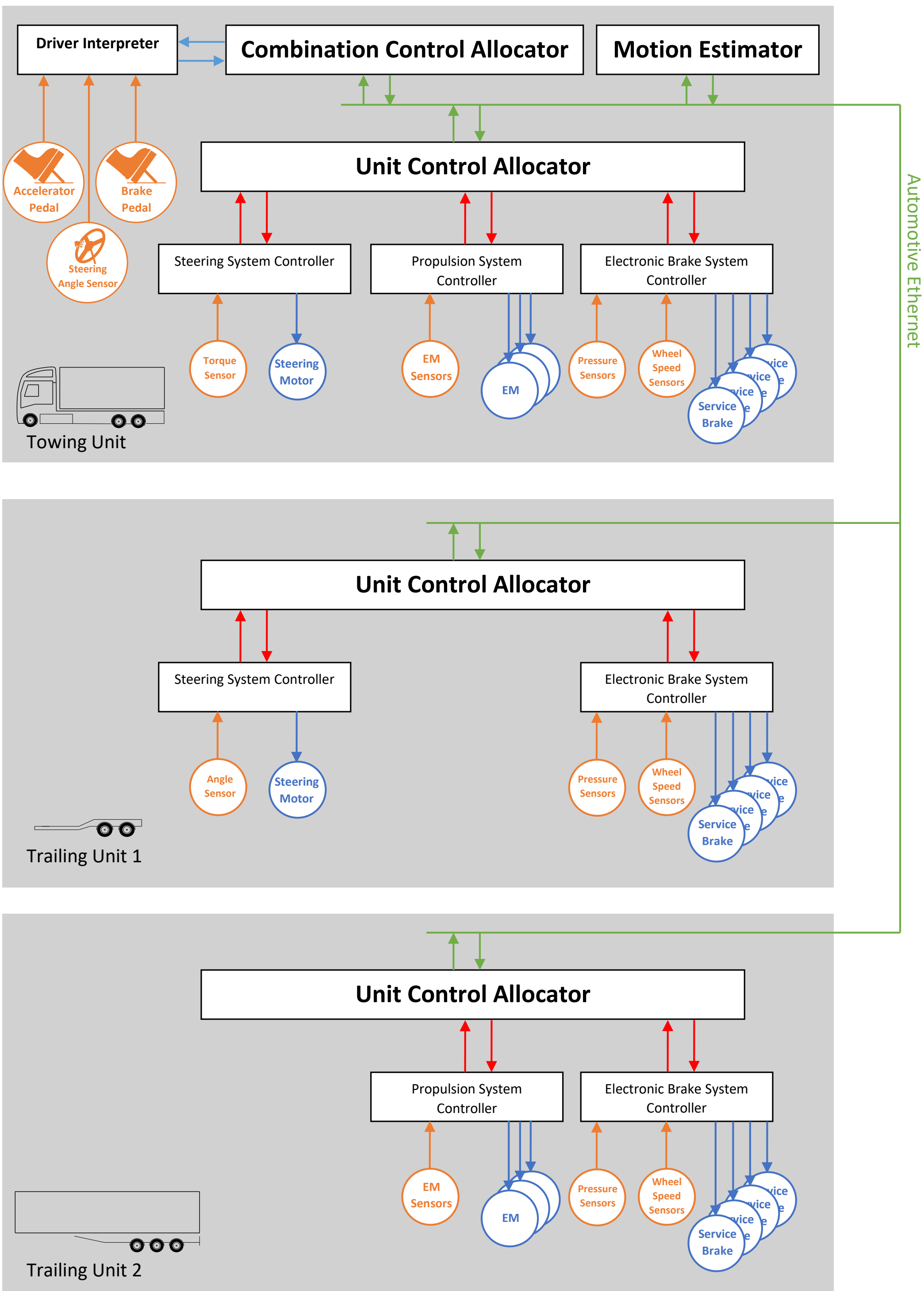

Figure 3.2: Envisioned functional architecture for heavy vehicle combinations

also be sent via a CAN network alternatively but requires a newer standard than the current ISO11992 which is optimized for the electrified vehicle combinations.

Table 3.1: Envisioned signal interface to and from the combination control allocator

Signal	Req.	Stat.	Cap.	from	to
Longitudinal acceleration req.	✓			DI	CCA
Longitudinal acceleration		✓	✓	CCA	DI
Curvature req.	✓			DI	CCA
Curvature		✓	✓	CCA	DI
Total unit service brake force req.	✓			CCA	UCA
Total unit service brake force		✓	✓	UCA	CCA
Total unit electric motor force req.	✓			CCA	UCA
Total unit electric motor force		✓	✓	UCA	CCA
Steering angle req.	✓			CCA	UCA
Steering angle		✓	✓	UCA	CCA
Unit lumped EM power loss map		✓		UCA	CCA
Unit mass		✓		ME	CCA
Unit non-driven axles normal load		✓		ME	CCA
Unit driven axles normal load		✓		ME	CCA
Unit longitudinal velocity		✓		ME	CCA
Unit lateral velocity		✓		ME	CCA
Unit longitudinal acceleration		✓		ME	CCA
Unit lateral acceleration		✓		ME	CCA
Unit yaw rate		✓		ME	CCA
Unit side-slip angle		✓		ME	CCA
Unit articulation angle		✓		ME	CCA
Unit coupling force		✓		ME	CCA
Road friction		✓		ME	CCA

In the envisioned functional architecture and signal interface proposed in this section, a steer-by-wire system is considered. Hence, the DI receives the steering wheel angle input and converts it to a curvature request sent to the CCA. The CCA allocates the road wheel steering angle (or steering angle rate) requests into different units. If the steering system is not a steer-by-wire type, then the steering angle sensor can also be read by the local steering system controller of the tractor, the CCA cannot request a steering angle from the truck CCA, but instead, the steered angle is directly controlled by the driver manually. The steering system controller in the truck can still apply additional torque to the steering column for driver assistance systems. In the case of an active steering system in trailing units, the CCA can still request steering angles of the trailing units. If there are multiple steered axles in the units, the CCA can alternatively request a lateral force or curvature from the UCA. Then UCAs allocate the steering angles to various steered axles. In another alternative, the CCA can request an equivalent (lumped) steering angle considering a kinematic vehicle model and the UCA allocates the steering angles to each steered axle locally. The steering coordination at the combination level via the CCA can bring advantages such as improved stability, reduced swept path, and improved maneuverability. Additionally, lateral dynamics is not influenced only by the steering but also by differential braking or propulsion. Therefore, coordinating steering, braking, and propulsion together can further improve these advantages. However, it is important to note that steering control is beyond the scope of this study.

The CCA may receive requests from a predictive energy management (PEM) controller instead of a DI. The PEM controller can consider the upcoming road profile, such as the next 10 km, and optimize energy consumption. In this study, however, only instantaneous control is considered.

Chapter 4

Unsafe modes of articulated heavy vehicles

In recent years, longer combinations with multiple articulation points have become more common due to their commercial and environmental benefits. In general, these vehicles tend to exhibit motion instabilities, such as jackknifing, trailer swing, combination spin-out, trailer sway, and rollover. The first four relate to the yaw degree of freedom, and the last one relates to the roll degree of freedom. Jackknifing and trailer swing happen when the towing or trailing units lose their lateral grips, usually due to too large braking or propulsion forces and locked wheels at slippery conditions. Combination spin-out is defined as a combination of the aforementioned two instability modes, resulting in all units of the combination sliding sideways. Trailer sway, on the other hand, is a more dynamic problem and relates to the rearward amplification of multiple units. The lateral velocity or yaw rate of the trailing units is amplified compared to the towing unit and may result in catastrophic accidents. Finally, rollover happens at high lateral accelerations if the center of gravity of the payload is high. In this chapter, these motion instabilities are explained in detail.

4.1 Jackknifing

Jackknifing is defined as the loss of directional stability of the towing unit. This results in having excessive articulation angle and a large heading angle deviation of the towing unit from the intended direction of travel. It happens when the towing unit loses lateral tire grip and starts to slide sideways. Losing lateral tire grip is typically caused by having excessive combined tire slip that happens during braking or propelling in a turn. A typical jackknifing of an AHV is illustrated in Fig. 4.1.a. The tractor and semitrailer are depicted by the blue and gray units, respectively.

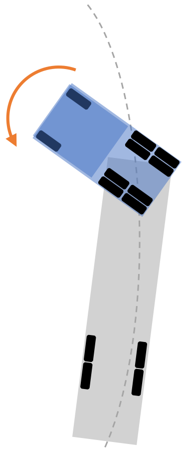

(a) Illustration of jackknifing of an AHV

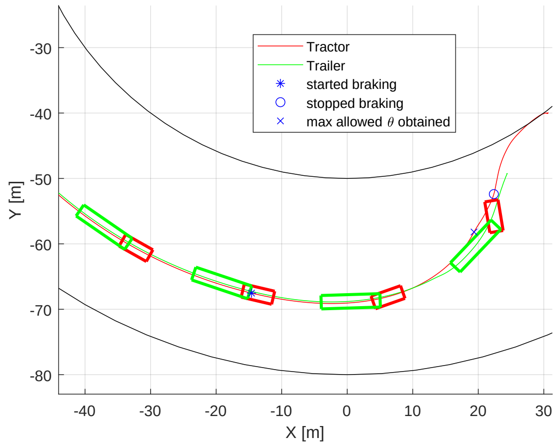

(b) Path of an AHV during a brake-in-turn test leading to jackknifing

Figure 4.1: Illustration of jackknifing and the corresponding path

In Fig. 4.1.b, the path followed by a real tractor-semitrailer combination during a brake-in-turn test is illustrated. The tractor is braked extensively with the drive axle at the point marked with the blue asterisk. This results in the activation of the slip controller and thus brake forces are limited. After braking, the AHV exhibits jackknifing, the tractor loses grip at the drive axles, and starts to slide sideways, and then the articulation angle grows in an undesired way.

In Fig. 4.2, the most important states of the tractor and semitrailer are depicted. Braking starts at the point marked by the first vertical solid line, and the driver keeps the steering angle constant during the braking. Braking is stopped when the test vehicle is about to leave the test track, indicated by the second vertical solid line. The key conclusions drawn from the states are listed as:

- The yaw rate of the tractor is growing quickly, while the semitrailer's yaw rate is rather close to the quasi-steady-state value (which is the value before the vertical line).

- The articulation angle grows substantially. As the vehicle is equipped with jackknifing protection cables, the articulation angle is limited with 60° and when it reaches the limit (shown with the dashed line), cables get tight and prevent the vehicle from having a catastrophic jackknifing (semitrailer hitting the tractor cab).

- Although the semitrailer keeps the side-slip angle similar to the quasi-steady-state value, the tractor's side-slip angle grows extensively.

If a timely intervention is not applied, jackknifing can result in the tractor cabin hitting the semitrailer, potentially leading to fatal accidents. Decreasing the propulsion or brake forces, or applying a corrective yaw moment via differential braking can help to avoid jackknifing. Trucks and tractors have Electronic Stability Control (ESC) which detects yaw instabilities and takes preventive actions like differential braking to apply corrective yaw moment.

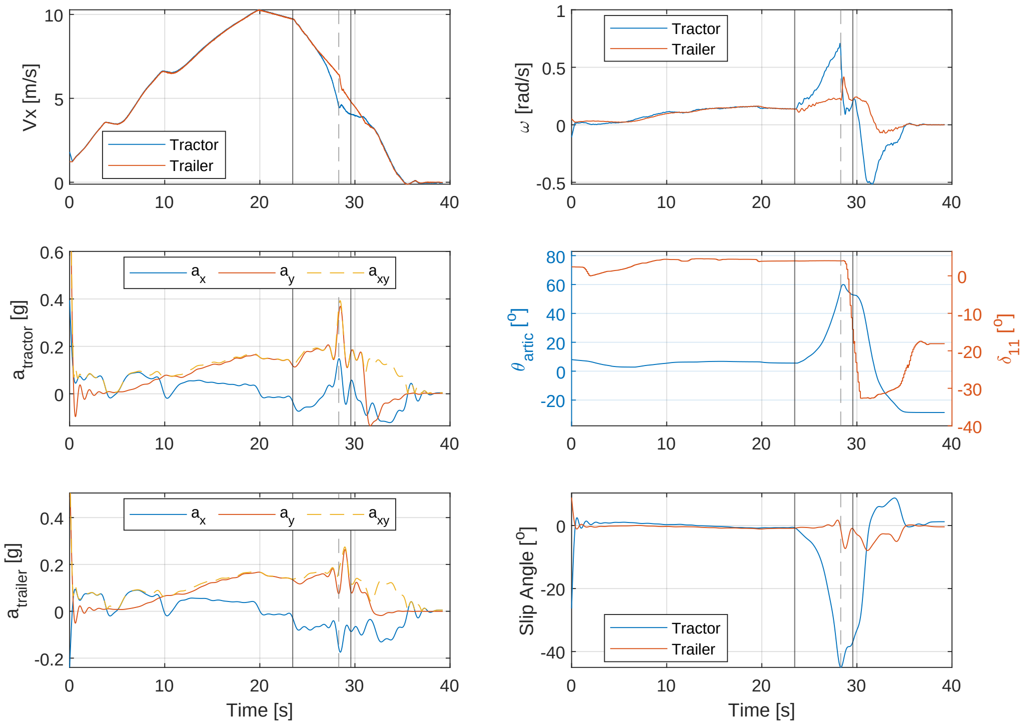

Figure 4.2: Longitudinal velocity V_x, longitudinal acceleration a_x, lateral acceleration a_y, total acceleration a_{xy}, yaw rate ω, articulation angle θ_{artic}, front axle road wheel angle δ_{11} and side-slip angles of the tractor (measured at the midpoint of the drive axles) and semitrailer (measured at the midpoint of the semitrailer axle group) during a brake-in-turn test that resulted in jackknifing. Two vertical solid lines show the times braking started and stopped. The dashed vertical line shows when the maximum allowed articulation angle is reached.

4.2 Trailer swing

Trailer swing is defined as the loss of directional stability of the trailing unit, resulting in an excessive articulation angle and a large heading angle deviation of the trailing unit from the intended direction of travel. This happens when the trailing unit loses lateral tire grip and starts to slide sideways. Losing the lateral tire grip is typically caused by excessive combined tire slip, which happens during braking or propelling in a turn. A typical trailer swing of an AHV is illustrated in Fig. 4.3.a.

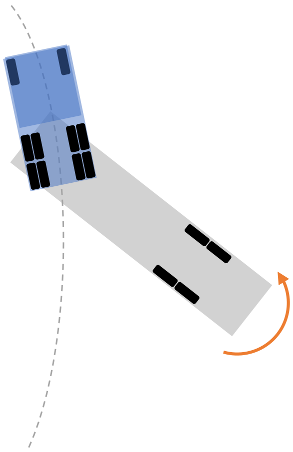

(a) Illustration of trailer swing of an AHV

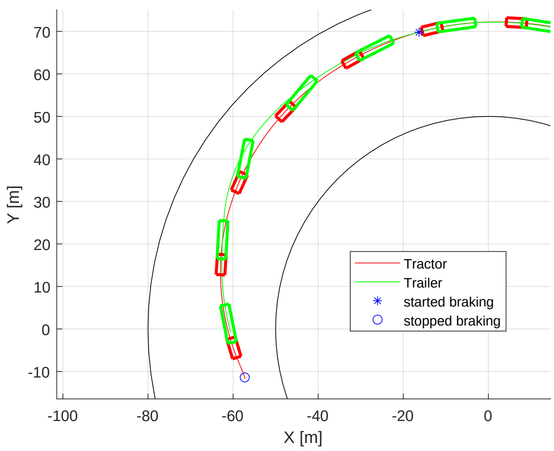

(b) Path of an AHV during a brake-in-turn test leading to trailer swing

Figure 4.3: Illustration of trailer swing and the corresponding path

The trajectory of a real tractor-semitrailer combination during a brake-in-turn test is depicted in Fig. 4.3.b. The semitrailer is braked extensively at the marked point shown with the blue asterisk, leading to activation of the slip controller and thereby limiting brake forces. After the braking point, the AHV experiences a trailer swing, and the semitrailer loses its grip and starts to slide sideways, and then the articulation angle grows in an undesired way.

The most significant states of the tractor and semitrailer are depicted in Fig. 4.4. Braking starts at the moment marked by the first vertical solid line and the driver keeps the steering angle constant during braking until coming to a standstill, indicated by the second vertical solid line. The key conclusions drawn from these states are listed as:

- The yaw rate of the semitrailer is growing quickly while the tractor's yaw rate is decreasing due to braking. However, after some time, the semitrailer's yaw rate also begins to decrease, becoming smaller than the tractor's yaw rate. Eventually, the semitrailer's yaw rate increases again, approaching the tractor's yaw rate. This rise and decrease in the trailer yaw rate are due to the semitrailer swinging first but then returning to the stable position.

- The articulation angle grows significantly and then it goes back to the quasi-steady-state value, which corresponds to the value at the moment the vehicle starts to brake, indicated by the first vertical black line.

- Although the tractor maintains the side-slip angle almost similar to the quasi-steady-state value, the semitrailer's side-slip angle grows substantially. However, as the yaw rate of the semitrailer decreases faster than that of the tractor after some time, the semitrailer's side-slip angle begins to decrease and eventually becomes similar to the tractor's side-slip angle.

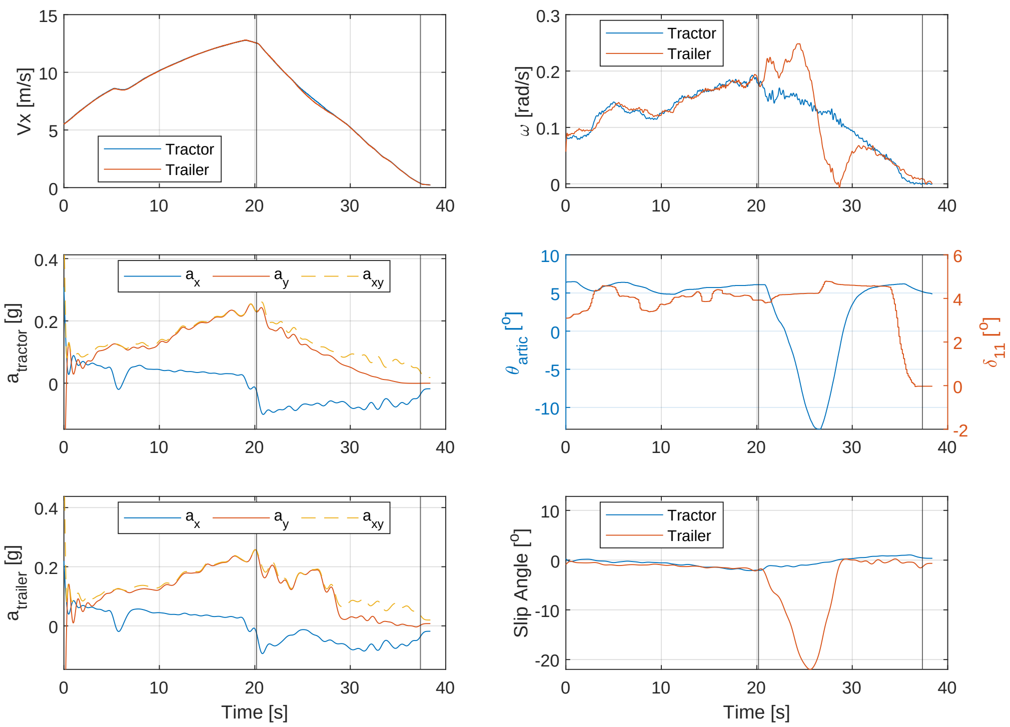

Figure 4.4: Longitudinal velocity V_x, longitudinal acceleration a_x, lateral acceleration a_y, total acceleration a_{xy}, yaw rate ω, articulation angle θ_{artic}, front axle road wheel angle δ_{11} and side-slip angles of the tractor (measured at the midpoint of the drive axles) and semitrailer (measured at the midpoint of the semitrailer axle group) during a brake-in-turn test that resulted in trailer swing. Two vertical solid lines show the times braking started and stopped.

Real tests have shown that the severity of trailer swing during braking may decrease over time due to decreasing speed, unlike jackknifing. Nevertheless, it is important to avoid an excessive trailer swing, before the trailer leaves the lane and potentially collides with vehicles in adjacent lanes, by decreasing the brake or propulsion forces.

Trailers typically have no yaw stability controllers like Electronic Stability Control (ESC) found in towing trucks and tractors to avoid trailer swing. However, trailers are equipped with ABS, which helps preventing excessive wheel slip and hence decreases the risk of trailer swing.

4.3 Combination spin-out

Combination spin-out, in this study, is defined as the loss of directional stability in both towing and trailing units simultaneously. Unlike jackknifing or trailer swing, the articulation angle may not grow significantly as both of the units have large heading angle deviations from the intended direction of the travel. Combination spin-out happens when both towing and trailing units lose their lateral tire grip and start to slide sideways. Losing the lateral tire grip is typically caused by having excessive combined tire slip, which occurs during braking or propelling in a turn. A typical combination spin-out of an AHV is illustrated in Fig. 4.5.a.

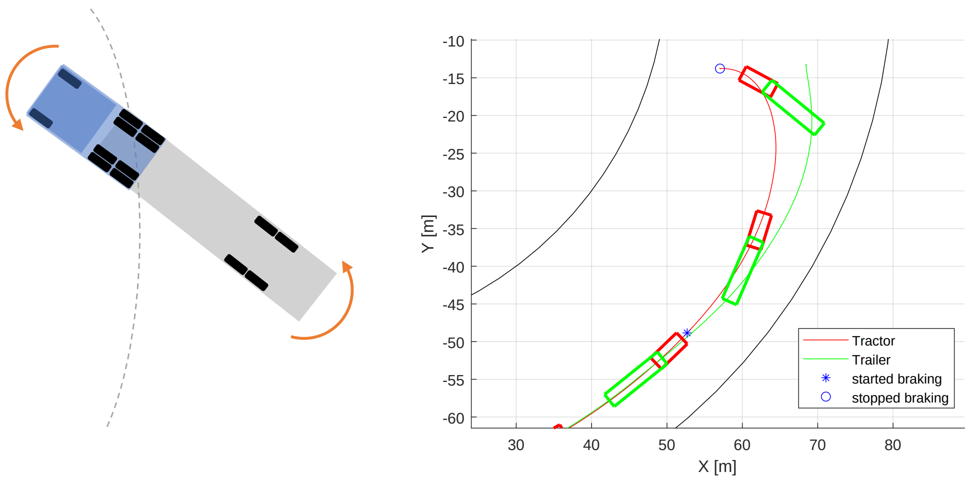

(a) Illustration of combination spin-out of an AHV

(b) Path of an AHV during a brake-in-turn test leading to combination spin-out

Figure 4.5: Illustration of combination spin-out and the corresponding path

In Fig. 4.5.b, the trajectory of a real tractor-semitrailer combination during a brake-in-turn test is illustrated. Both units are braked extensively at the point indicated by the blue asterisk. After the braking point, the AHV exhibits a combination spin-out, causing both units to lose their grip and start to slide sideways.

The key states of the tractor and semitrailer are depicted in Fig. 4.6. Braking begins at the moment indicated by the first vertical solid line, and the driver keeps the steering angle constant throughout braking until coming to a standstill, represented by the second vertical solid line. The yaw rates of both units increase together and decrease after some time, leading to high side-slip angles in both units. As the yaw rates of two units grow and decrease together, the articulation angle doesn't increase as much as in the cases of jackknifing or trailer swing. Nevertheless, the articulation still grows to a moderate value since the yaw rates of the two units do not follow exactly same trend.

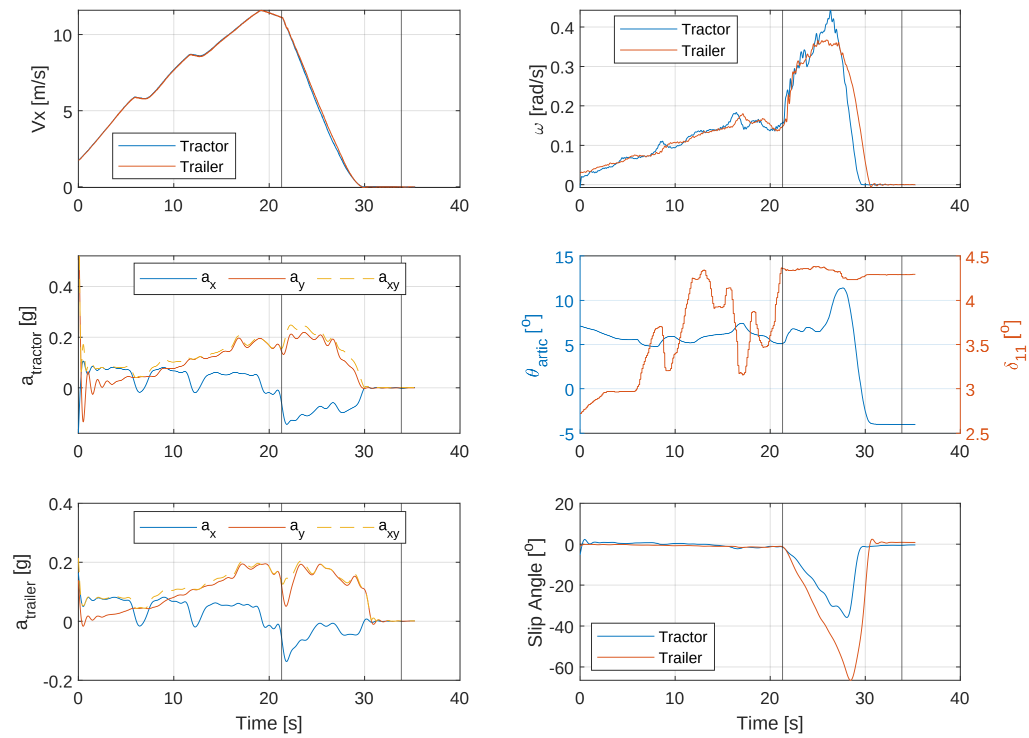

Figure 4.6: Longitudinal velocity V_x, longitudinal acceleration a_x, lateral acceleration a_y, total acceleration a_{xy}, yaw rate ω, articulation angle θ_{artic}, front axle road wheel angle δ_{11} and side-slip angles of the tractor (measured at the midpoint of the drive axles) and semitrailer (measured at the midpoint of the semitrailer axle group) during a brake-in-turn test that resulted in combination spin-out. Two vertical solid lines show the times braking started and stopped.

The growth of the articulation angle during a combination spin-out depends on the respective magnitudes of the tractor's and the semitrailer's yaw rates. As in the real tests, the surface friction varies heterogeneously among the test area, it is not possible to claim that the combination vehicle will always turn like a single rigid body without too much growth in the articulation angle. If the tractor has a larger yaw rate for some time, then the articulation angle will grow with the same sign of the yaw rate, as in the case of jackknifing, and jackknifing will be the dominant mode compared to the trailer swing. If the semitrailer has a larger yaw rate for some time, then the articulation angle will grow with the opposite sign of the yaw rate, as in the case of trailer swing, and trailer swing will be the dominant mode compared to the jackknifing. Alternatively, if the yaw rates of both units grow at a comparable rate and stay close to each other, then the articulation angle will not grow, and the AHV will have a yaw motion like a single rigid body, turning around a yaw center as a whole combination.

4.4 Trailer sway

Yaw instabilities explained so far are divergent instabilities that involve one or several motion states (such as yaw rate) growing without oscillations. However, the states of a vehicle may experience oscillatory behavior and even grow with oscillations which is called "dynamic instability". Trailer sway is a dynamic instability that relates to the yaw dynamics of the combination.

Rearward amplification (RA) refers to the ratio between the maximum values of a lateral dynamics state observed in the first and last units of a combination. The state is typically chosen as the lateral acceleration or yaw rate. RA is used as a criterion to evaluate the risk for a rollover or swing-out of the last unit compared to what is experienced by the driver [22]. The maximum RA allowed for the vehicle combinations in Sweden is 2.4 [23]. Investigation of RA is usually done with lane change maneuvers or sinus-wave-shaped steering inputs.

Kharrazi et al. investigated the RA of yaw rate for many different AHV combinations and obtained the RA as 2.12 for truck-double center axle trailer combination, A-double as 1.84, Nordic combination as 1.65, AB-double as 1.65, tractor-semitrailer as 1.08 [24]. Hence, the riskiest long combination is truck-double center axle trailers.

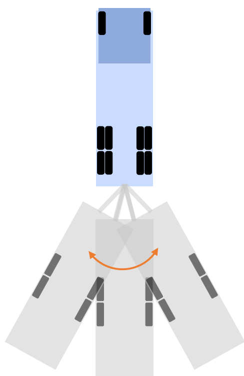

Figure 4.7: Illustration of trailer sway. The trailing unit (gray) continuously sways sideways around the coupling.

Evaluating dynamic stability only with RA is not always sufficient. Yaw damping, defined as the damping of lateral excitation over time, decreases for higher speeds. If the yaw damping of a combination reaches zero at a certain high speed (defined as zero-damping speed), lateral oscillations will not be dampened over time, leading to self-excitation and continue to increase. Combinations with no center-axle trailer would normally have sufficient yaw damping [25]. Combinations with center-axle trailers, on the other hand, may become self-excited over a certain speed with insufficient yaw damping due to improper loading, coupling distances, and wheelbases. An example of this scenario, where the corresponding combination exceeds the zero-damping speed of 89 km/h, is depicted in Fig. 4.8 [25]. In this case, the yaw rates of the units keep increasing after a lane change since there is not enough yaw damping.

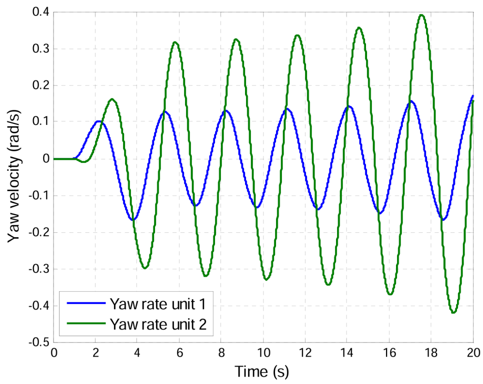

Figure 4.8: Self-excited yaw velocity response for a 6x4 truck and center axle trailer [25]

Combinations exceeding the zero-damping speed continue to sway even after a small excitation, for example, due to a lane change or side wind. This swaying continues if not taken under control by employing, for example, a corrective yaw moment with differential braking, or stretch braking. For passenger cars towing small trailers or caravans, there are several stability control systems that corrective actions may be applied by the towing unit (such as Toyota Trailer Sway Control system with differential braking, TSC [26]), or trailing unit (such as Bosch Trailer Safety Control system with differential braking, TSC [27], or AL-KO Trailer Control system with stretch braking, ATC [28]). If the self-excitation is not taken under control on time, trailer sway can lead trailers to roll over, or result in very large swept path, eventually leading to folding of the combination like jackknifing [29].

4.5 Rollover

An important instability mode of heavy vehicles is rollover, which typically occurs in vehicle combinations with a high center of gravity, such as timber trailers, tankers, or concrete mixers. Rollover usually occurs during maneuvers involving high lateral accelerations, such as sharp turns or lane changes. However, it can also happen under static conditions at a standstill due to high bank angles or large side winds.

During dynamic maneuvers with high lateral accelerations, rollover typically starts at the trailers, causing the inner wheels of the trailer to lift off. Subsequently, the towing units also roll over as a continuation. Since the trailers are not very stiff in the roll direction due to their long wheelbases, rollover may progressively happen starting from the rear end of the combination towards the front. Even though rollover usually begins from the trailers due to their high center of gravity and mass, and then affects the towing units; it may also first happen on the towing units with high centers of gravity, like rigid trucks, especially during clothoid maneuvers with progressively increasing turning radius, since the towing units experience a higher lateral acceleration compared to the trailing units. Figure 4.9 illustrates a tractor-semitrailer combination experiencing rollover [30].

Figure 4.9: A tractor-semitrailer combination rolling over during electric truck crash safety tests [30]

Modern trucks and trailers are often equipped with Roll Stability Controllers (RSC). These controllers brake the combination to reduce the speed which eventually reduces the lateral acceleration. Some passenger cars are equipped with active rollover prevention systems that observe the states of the vehicle to avoid rollover by utilizing active suspensions and roll-bars [31], or braking a subset of the wheels to lose the lateral grip and consequently reduce lateral forces acting on the vehicle [32]. Additionally, there are further studies exploring rollover prevention via active steering [33].

Chapter 5

Safe operating envelope

Traditional heavy vehicle combinations have internal combustion engines only in the towing unit, making it trivial to control the propulsion and braking forces. For propelling the combination, the driver's request is received from the accelerator pedal and a simple control strategy is applied to control the engine torque. Service brake request received by the brake pedal, on the other hand, is fulfilled through the braking forces proportional to axle loads which is the safest allocation for vehicle stability. When retarders are used, brake blending is performed between the engine's exhaust brake, retarder, and service brakes. With the electrification of both towing and trailing units in heavy vehicle combinations, novel control allocation strategies for distributing the propulsion and regenerative braking forces to different units are needed. These strategies should minimize energy consumption considering the efficiency maps of various electric motors and other power losses. Meanwhile, the controller should ensure the distribution of the actuator requests safely. If too much force is allocated to the leading unit, a jackknifing may happen. If an excessive force is allocated to the trailing unit, a trailer swing can occur. To ensure safe allocation, a Safe Operating Envelope (SOE), also known as Maneuvering Limitation Diagram (MLD), safe maneuvering envelope, or safe set, can be utilized. It is defined as a set of operational limits and conditions of the vehicle states and actuator requests for a safe vehicle operation. A control allocation performed by utilizing the SOE increases safety and reduces the risk of instabilities such as jackknifing and trailer swing. Furthermore, the SOE is an important diagram for understanding vehicle combination instabilities and safety limits. An accurate vehicle dynamics model, such as a two-track model, can be used to generate a precise SOE. Once validated through high-fidelity simulations or real tests, this model then becomes a suitable candidate to be integrated into a model-based control design, such as model predictive control.

5.1 Safe operating envelope in force domain

Safe Operating Envelope (SOE) is defined as a set of safe limits on actuator requests and formulated as a function of vehicle states (such as lateral acceleration) and environmental parameters (such as road friction coefficient). In **Paper A**, SOEs for both propulsion and braking are obtained as a function of normalized lateral acceleration, c_y, which is defined as:

$$c_y = \frac{a_y}{\mu g} \tag{5.1}$$

where a_y is the lateral acceleration of the towing unit, μ is the friction coefficient, and g is the gravitational acceleration.

For each c_y, hence for different combinations of road frictions and lateral accelerations, a 2-dimensional SOE is obtained by simulating brake-in-turn or propel-in-turn maneuvers with many various combinations of tractor and semitrailer actuator forces. In the simulations, a single-track model is employed. Tire forces are limited with respect to the corresponding friction circles [34]. The applied propulsion or braking forces, F_{1rx} for the tractor drive axle and F_{2x} for the semitrailer's axle group, are defined as:

$$\begin{cases} F_{1rx} & = & c_{tractor} \cdot \mu \cdot F_{1rz} \\ F_{2x} & = & c_{trailer} \cdot \mu \cdot F_{2z} \end{cases} \tag{5.2}$$

where F_{1rz} and F_{2z} are the normal loads on the tractor's drive axle and the semitrailer's axle group, respectively. $c_{tractor}$ and $c_{trailer}$ denote the friction utilization coefficients for the tractor and semitrailer, respectively. By varying these coefficients in the interval of [-1,0] for braking and [0,+1] for propulsion, each maneuver is classified as safe or unsafe. For defining a safe maneuver, the following criteria are used:

$$\max(\Delta\beta_{1r}) < 5^\circ \;\; \& \;\; \max(\Delta\beta_2) < 3^\circ. \tag{5.3}$$

where $\max(\Delta\beta_{1r})$ denotes the maximum deviation of the side-slip angle of the tractor's drive axle from its quasi-steady-state value, and $\max(\Delta\beta_2)$ represents the same for the semitrailer axle group. Quasi-steady-state side-slip angles are the values of these states just before the application of actuator forces, describing a well-behaving and stable combination. For a semitrailer with a length of 10 m, a limit of 3° side-slip angle deviation results in approximately 0.5 m lateral displacement. This limit is chosen to avoid a larger lateral displacement which could cause the semitrailer to leave its lane and collide with other vehicles in adjacent lanes. For the tractor, a larger limit of 5° is chosen since towing units are shorter than trailing units and can tolerate a larger side-slip angle deviation without leaving the lane.

A generic 2-dimensional SOE for a specific c_y is shown in Fig. 5.1 for a braking tractor-semitrailer combination. Typically, above a certain level of $c_{trailer}$, trailer swing occurs. This limiting $c_{trailer}$ has a small correlation with tractor forces, which means, trailer swing happens almost regardless of how much the tractor is braking or propelling. Similarly, beyond a certain level of $c_{tractor}$, jackknifing occurs. Jackknifing, unlike trailer swing, is more probable when the semitrailer is not braked, which is reflected by the inclined limit for jackknifing in Fig. 5.1. Therefore, braking the semitrailer helps to prevent jackknifing up to a certain level, by introducing a corrective yaw moment on the towing unit. This feature, known as "stretch braking", is applied in heavy vehicle combinations traveling downhill slopes by braking the trailer, to enhance vehicle safety. In the case of propulsion, on the other hand, applying less propulsion with the semitrailer helps to avoid tractor jackknifing. The common characteristic of the two cases is that a larger tension force in the coupling enhances the yaw stability of the towing vehicle.

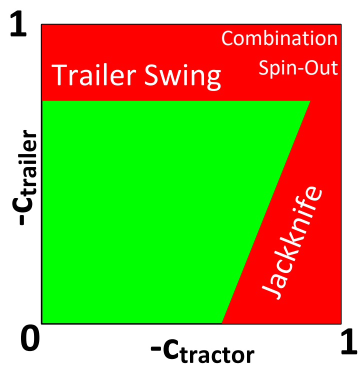

Figure 5.1: Different yaw instability modes shown on the SOE for a braking vehicle combination. From Paper A.

For combinations of the larger (in the absolute sense) values of $c_{tractor}$ and $c_{trailer}$, a combination spin-out happens, indicating instability in both the towing and trailing units.

In **Paper B**, a high-fidelity model called as Volvo Transport Model (VTM) [35] is employed to derive the SOE of a tractor-semitrailer combination. This simulation model also incorporates a simple slip controller for keeping the wheel slips under control. Numerous simulations are conducted for a brake-in-turn maneuver to obtain an SOE, as shown in Fig. 5.2.

Simulations are conducted for four different c_y values, and a 2-dimensional SOE is obtained for each c_y as depicted in Fig. 5.2a. For smaller lateral accelerations, all combinations of tractor and semitrailer braking forces are identified as safe (shown in green). For higher lateral accelerations, on the other hand,

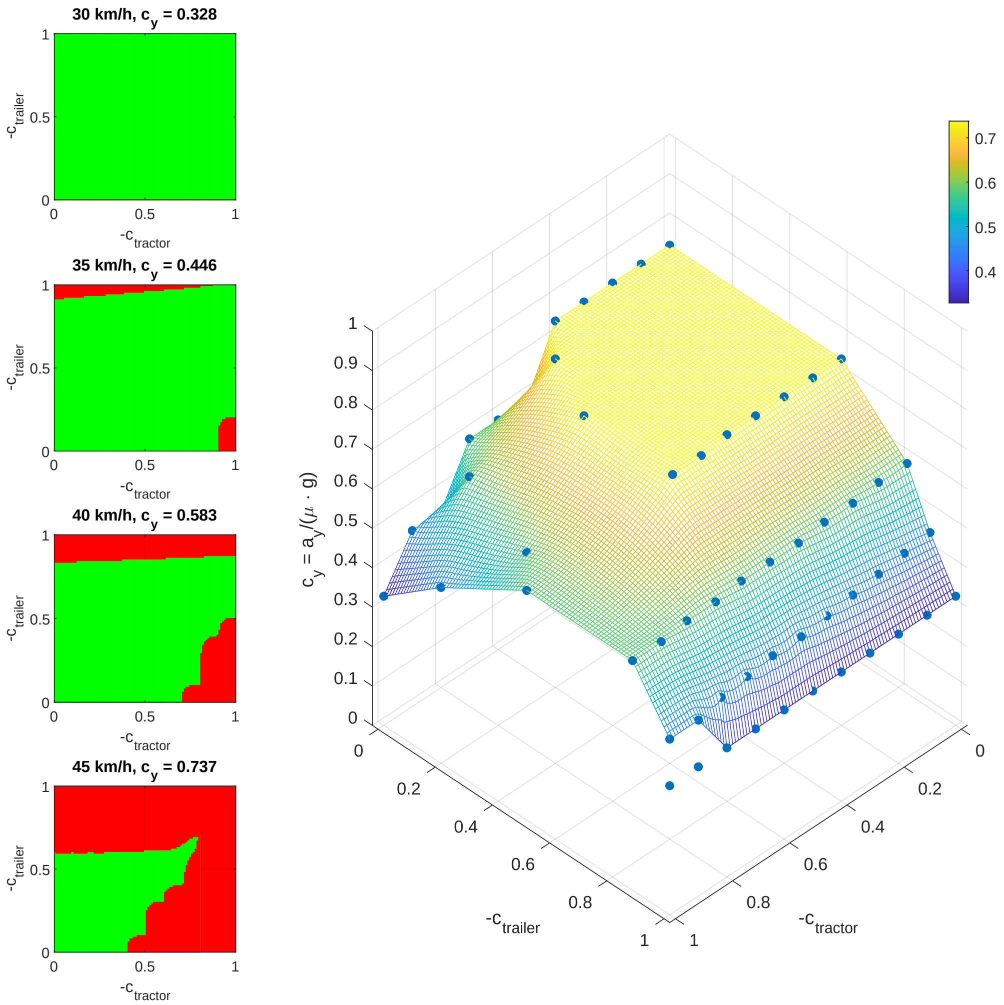

(a) (b)

Figure 5.2: SOE obtained from the high-fidelity simulations for a tractor-semitrailer combination braking-in-turn. Adapted from Paper B.

excessive braking forces result in yaw instabilities such as jackknifing and trailer swing (shown in red). The 2-dimensional SOEs are used to derive a 3-dimensional SOE, as presented in Fig. 5.2b, where the vertical axis represents c_y. Envelopes for the intermediate c_y values that are not simulated are interpolated, hence a 3-dimensional surface is obtained. The maximum c_y value simulated is 0.737, corresponding to the highest speed (45 km/h) that the combination can reach for the simulated turning radius of 72 m, friction coefficient of 0.3, and loading conditions. Any combination of c_y, $c_{tractor}$ and $c_{trailer}$ values under the obtained SOE surface results in a stable maneuver, and any combination of those above the SOE surface results in an unstable maneuver, leading to a jackknifing, trailer swing, or combination spin-out. The SOE obtained with high-fidelity model simulations is validated with real vehicle tests.

In **Paper C**, an alternative two-track model with roll dynamics is presented to obtain an SOE. This model also incorporates a friction-circle-inspired combined slip model that is lacking in the single-track model presented in Paper A. SOEs obtained with single-track and two-track models are compared with the SOE obtained with high-fidelity simulations. All SOEs for four different speeds (and c_y values) with three different models are shown in Fig. 5.3.

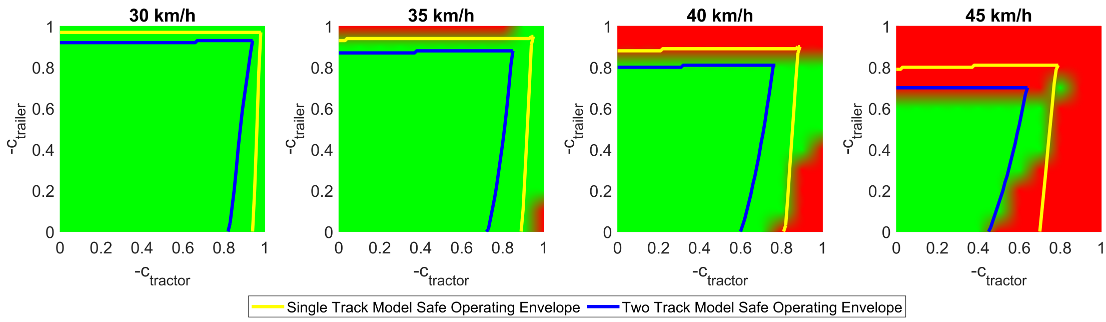

Figure 5.3: SOEs obtained with single-track model (yellow line), two-track model (blue line) and high-fidelity VTM model with slip controller (red/green background). From Paper C.

It is shown that a two-track model with roll dynamics, lateral load transfer, and combined slip model outperforms the single-track model in terms of the accuracy of the SOE compared to the one obtained from high-fidelity model simulations. Therefore, the combined slip model for simulating large tire forces close to the tire limits, and the inclusion of lateral load transfer due to higher lateral accelerations, are important when deriving an SOE. The SOE obtained from the two-track model closely matches the one obtained from the VTM with no slip controller (which is a fairer comparison compared to VTM with slip controller, since the two-track model also lacks the slip controller). In Fig. 5.3, as VTM is simulated with a slip controller (which is more realistic scenario since the modern vehicles are equipped with ABS), SOE obtained with the two-track model is smaller in lower lateral accelerations compared to the one obtained with the VTM. However, this is due to the slip controller in the high-fidelity model lowering the brake forces and leaves enough lateral force capability for maintaining yaw stability. The two-track model, on the other hand, has no slip controller, but the lateral tire forces are limited with respect to the friction circle, which results in a smaller lateral force capability to maintain yaw stability. Nevertheless, the SOE obtained with two-track model is more conservative and is mostly smaller than the SOE obtained with the VTM as shown in Fig. 5.3. Thus, using this SOE in the vehicle control would result in a safe control allocation.

The SOE obtained from any of these methods can serve as inequality constraints in the control allocation formulation as demonstrated in Section 2.5. Alternatively, the two-track model, validated against a high-fidelity model, can be employed in a model-based controller, such as Model Predictive Control (MPC). The model can be simulated with a receding time horizon (e.g., 2 seconds) and safety constraints on certain vehicle states (such as yaw rate or side-slip angle) can be implemented to ensure the combination's stability.

5.2 Safe operating envelope in slip domain

An alternative approach for defining a safe operating envelope for the combination is utilizing the slip limits on the units, instead of forces. It is possible to generate phase plane trajectories of the combination vehicles for a set of specific operating conditions (e.g., friction, payload, etc.). These phase plane trajectories can be plotted for different sets of states: such as side-slip angle versus side-slip angle rate [36], lateral velocity versus yaw rate [37] or side-slip angle versus yaw rate [38].

In Fig. 5.4, a phase plane trajectory for a coach is shown [36], focusing on side-slip angle and side-slip angle rate. The upper and lower boundaries for vehicle stability are shown with red lines. The domain of attraction lies in between these red lines, where the vehicle is stabilized over time. Outside of these boundaries, on the other hand, the domain of repulsion takes place, where the vehicle's side-slip angle grows and eventually the grip is lost and vehicle becomes unstable.

For multi-unit vehicles, generating such envelopes is also possible, although it is more complicated compared to single-unit vehicles. This complexity is due to the interdependency of states among different units, hence there might be multiple envelopes. In other words, e.g., the phase plane trajectory of the tractor may vary for different yaw rates of the semitrailer. Nevertheless, an alternative approach to SOE in the force domain is using stability margin for the side-slip angle and expressing the SOE in the slip domain.

As modern electric vehicles have interfaces not only to control the motor torque but also to limit or control the motor slips or speeds, the SOE in a side-slip domain can further be extended to cover the longitudinal slips. In Fig. 5.5, lateral forces as a function of longitudinal slip for a number of constant vehicle side-slip angles are depicted. It is observed that for larger side-slip angles, the lateral force generated by the tires decreases significantly if a large longitudinal slip is present. Hence, it is important to limit the longitudinal slip of the electric motors, when a large lateral force is needed to maintain yaw stability in high lateral accelerations, especially

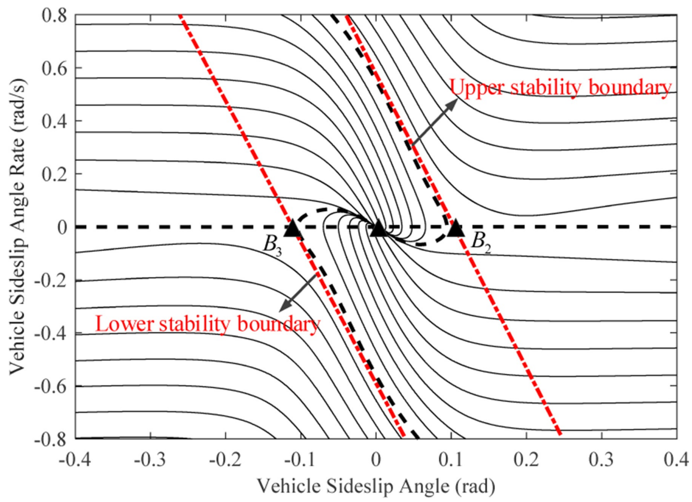

Figure 5.4: Vehicle side-slip angle versus side-slip angle rate phase plane trajectory for a coach [36]

on surfaces with lower road frictions.

In **Paper E**, an SOE in the longitudinal slip limit versus side-slip angle domain is presented, referred to as ”slip polytope”, illustrated in Fig. 5.6. Although it is represented as a 2-dimensional envelope in the paper, it can have more dimensions. For instance, the longitudinal slip limit of the tractor electric motors may be determined not only as a function of the tractor side-slip angle but also, for example, the semitrailer yaw rate or side-slip angle.

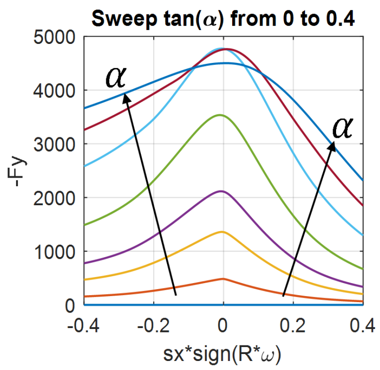

Figure 5.5: Lateral force F_y as a function of longitudinal slip S_x for a number of constant vehicle side-slip angles α [39]

In Fig. 5.6, the adaptive longitudinal slip limit, S_x^{lim}, is shown as a function of the deviation of the side-slip angle β from the reference side-slip angle β^{ref}. β^{ref} is estimated via a vehicle dynamics model for quasi-steady-state conditions. Therefore, β^{ref} represents the side-slip angle of the unit (or axle) for the specific

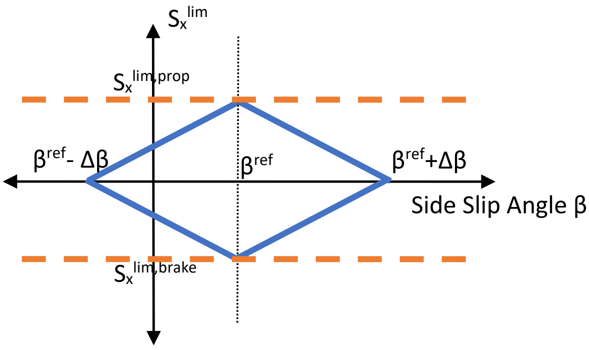

Figure 5.6: Longitudinal slip limit S_x^{lim} represented as a function of side-slip angle β deviation from the reference side-slip angle β^{ref}. Adapted from Paper E.

speed and turning radius, for zero longitudinal, and yaw acceleration, and with zero longitudinal forces on the wheels (no braking or propulsion). If the measured or estimated side-slip angle of the unit (or axle), β, is equal to β^{ref}, then positive and negative slip limits for the unit's electric motors are set as the default limits $S_x^{lim,prop}$ and $S_x^{lim,brake}$, respectively. These can typically be in the range of $\pm 5\%$ to $\pm 15\%$, depending on the conditions. Any deviation of the side-slip angle β from the reference side-slip angle β^{ref} results in a reduction in the longitudinal slip limit S_x^{lim}. A side-slip angle deviation of $\Delta\beta$ reduces S_x^{lim} to 0, indicating that at this level of side-slip angle deviation, no longitudinal force can be applied by the actuators, and all the tire force capability is exclusively reserved for the lateral direction to maintain yaw stability. Although a simple linear decrease in the slip limits is exemplified in this study, a more advanced envelope can be applied to the slips, such as an ellipse, or a higher order polytope, possibly with a dead band around β^{ref} with no penalization for S_x^{lim} for small side-slip angle deviations. This slip envelope is applied to the electric motors of the units, but not to the service brakes. This means that service brakes are always available to slow down the vehicle. By imposing the slip polytope constraints, excessive regenerative braking with electric axles, or any propulsion that leads to yaw instabilities, can be avoided.

Chapter 6

Real-time control allocation with safety constraints

First Electronic Stability Controllers (ESC) are introduced to passenger cars in 1990s. Today, ESC systems have become standard not only in cars but also in heavy vehicles. ESCs can sense an ongoing yaw instability with the sensors like inertial measurement units, and prevent total loss of control and stabilize the vehicle, usually via individual braking. ESCs, on the other hand, are not standard in heavy trailers. Another instability mode that is more common in heavy vehicles is rollover. Modern trucks and trailers have Roll Stability Controllers (RSC) to avoid a catastrophic rollover. With the electrification of heavy vehicles and trailers, regenerative braking with only one axle or one unit became motivated due to energy efficiency concerns, unlike service braking which is traditionally performed by all axles and all units proportional to the normal loads. Furthermore, due to the electrification of the trailing units, propelling with only the trailers also became an option, which gives a higher risk of instability than propelling with the towing units. It is therefore important to allocate the propulsion and regenerative braking forces into different units and axles of the heavy combinations in an energy-efficient and safe way. Although ESCs may mitigate some of the yaw instabilities, control allocators should already request a safe set of forces that will not cause jackknifing or trailer swing due to excessive forces. Safe allocation becomes more important, especially on the roads with low friction, and high curvature, in which, ESC systems may not mitigate all possible instabilities. In this chapter, five different approaches for safe control allocation will be presented. All of these methods perform on the combination control allocation layer, aiming to safely allocate the forces into different units of the combination. In the control allocator of each unit, which is out of the scope of this chapter, there may be additional safety algorithms, which for example, can request differential braking like ESC, hence it becomes possible to adapt the ESC function in the control allocator. The *combination control allocator studied in this chapter only allocates the longitudinal forces into different units, hence it does not involve allocation of any yaw moment or lateral force. Nevertheless, it aims to allocate forces in a safe way that does not result in yaw instabilities. Some of the methods studied in this chapter are proactive, meaning that the instabilities are avoided before they happen. And some are reactive, which means that instability is mitigated after it starts to happen.*

6.1 Real-time control allocation with power loss minimization

In **Paper D**, control allocation on a real tractor-semitrailer combination is tested in a real-time controller. The tractor is electrified, and the semitrailer is conventional without electric propulsion. A power loss minimization algorithm, as explained in Section 2.4 is adopted. In this simple case, the optimization is trivial, since it will always request propulsion or regenerative braking forces from the only electrified unit: the tractor. This case, however, is usually riskier than having two electrified units since excessive forces on the tractor drive axles may lead to jackknifing.

When the tractor's electric motor capabilities are reached during regenerative braking, further braking is performed via service brakes. Power losses in the service brakes of the tractor and semitrailer are equal since all the braking energy is dissipated as heat in either case. This results in an equal amount of usage of the service brakes of both units. However, this is not ideal, since the tractor is already braking with the electric motors, and equal application of service brakes in both units results in an excessively braking tractor. As a result, the (compressive) coupling force may grow significantly, and on slippery roads with high curvature, a jackknifing may occur. To overcome this problem, a "coupling force enhancement function" is also presented, which allocates more service brake force to the semitrailer, until the total brake forces of each unit become proportional to their normal loads. Hence, after the electric motor capabilities are reached, a safer brake force allocation is performed.

The real brake-in-turn tests performed on the circular frozen lake tracks of Colmis Proving Ground [40] show that control allocation with power loss minimization, without any additional safety constraint, leads to jackknifing on roads with low friction and high curvature. Therefore, it is essential to implement a proper set of safety mechanisms to ensure the yaw stability of the combination.

6.2 Safety constraints

In this section, five different safety algorithms are presented. These algorithms are used with the power loss minimization algorithm explained in Section 2.4, either as inequality constraints as shown in (2.5), or simply as upper and lower bounds for the allocated forces like box-constraints, as discussed in Section 2.5.

6.2.1 Safe operating envelope

In **Paper D**, a Safe Operating Envelope (SOE), presented in Section 5.1 is used with the power loss minimization algorithm for brake-in-turn tests. When the tractor drive axles' friction utilizations reach to the boundaries defined by the SOE, the total brake force request is fulfilled by applying additional semitrailer braking by using its service brakes. After slowing down due to braking, the lateral acceleration drops. As the SOE is larger for lower lateral accelerations, the amount of regenerative braking with tractor's electric motors increases as the combination continues to brake. The brake-in-turn maneuver is completed and the combination comes to a standstill safely without experiencing a jackknifing thanks to the SOE. This method is proactive since SOE ensures a safe allocation and any yaw instability is prevented before it happens.

6.2.2 Limiting the longitudinal force capabilities based on lateral force estimates

In **Paper D**, a lateral tire force estimator is presented. The lateral tire forces are then used to limit the longitudinal force capabilities of each unit by considering a friction circle [34]. Hence, at higher lateral accelerations, a smaller amount of longitudinal actuator forces are allowed, since most of the tire force capability is used for lateral direction to keep the combination stable. Avoiding a yaw instability before it happens means that this method is also proactive like SOE. In brake-in-turn tests, this approach results in safe braking and coming to a standstill safely without a jackknifing risk. As the longitudinal force capability of the tractor's electric axle is reduced, the total braking force is fulfilled mainly with additional braking via semitrailer service brakes, and a small amount of tractor service braking.

6.2.3 Decreasing longitudinal force capability based on high longitudinal slip detection

In **Paper D**, a reactive safety algorithm that observes the longitudinal wheel slips and lateral accelerations of the units to detect an ongoing yaw instability is presented. Under high longitudinal slips and high lateral accelerations, the electric motor capability of the tractor is reduced to avoid jackknifing. Since the method is reactive, which means that the force capabilities are reduced only after the wheel slips grow, the yaw rate of the tractor increases more than the proactive methods. Neverthless, the high slip is detected in 0.65 seconds, and after reducing the force capabilities, the tractor yaw rate quickly drops in 0.5 seconds to a safe level, thus the combination comes to a standstill safely without any further instability. The total brake force request is fulfilled with additional braking mostly via the semitrailer service brakes and a smaller contribution from the tractor service brakes.

6.2.4 Decreasing longitudinal force capability based on high lateral slip detection

Instead of detecting yaw instability based on the longitudinal slips of the units, an alternative approach is observing the lateral slips of the units, as presented in **Paper D**. In this case, an ongoing yaw instability is detected if the lateral acceleration and the unit side-slip angles are high. If those states are beyond the predetermined thresholds, then the tractor's electric motor force capability is reduced, hence this method, similar to the previous method, is also reactive. After the reduction in the regenerative braking capability, additional braking is performed mainly with the semitrailer service brakes, and partially with the tractor service brakes. The tractor's yaw rate grows higher than the proactive methods but in 1 second, a high side-slip is detected, and in 0.5 seconds of detection, the yaw rate of the tractor is taken under control. This method, similar to other methods, results in safe braking in a slippery curve, and the combination can come to a standstill without experiencing a jackknifing.

6.2.5 Adaptive longitudinal slip limit as a function of lateral slip

An alternative approach to ensuring yaw stability involves limiting the wheel slips instead of limiting the EM forces, as discussed in Section 5.2. In **Paper E**, first, a slip polytope is introduced. Then it is tested in a high-fidelity simulation model of a tractor-semitrailer combination for propel-in-turn maneuvers on low-friction surfaces. A quasi-steady-state side-slip angle for the tractor is estimated via an estimator using a single-track model. Then longitudinal slip limit of the slip controller is reduced proportionally to the deviations from this reference slip angle. It is shown that a vehicle combination with such an adaptive longitudinal slip limit can accelerate to faster speeds on low friction surfaces in a stable way compared to a combination with a constant slip limit. The combination with a fixed limit experiences a jackknifing, while the combination with an adaptive slip limit preserves small side-slip angles.

The same scenario is also tested with a real vehicle combination on a circular ice track. The driver is instructed to steer the vehicle to maintain directional stability. With an adaptive slip limit, the combination can accelerate to a certain speed in a quite smooth way, without significant steering effort. With constant slip limits, on the other hand, the vehicle repeatedly starts to slide sideways, and the driver tries to counter-steer to take control back. In this case, high side-slip angles are observed, and steering effort is substantially higher than the case with adaptive slip limits, meaning that the driver should significantly counter-steer and adapt the steering angle considering the body side-slip of the tractor. In the case of a constant slip limit, the vehicle cannot accelerate to higher speeds due to losing traction.

Chapter 7

Conclusions and future outlook

In this final chapter, conclusions are drawn and recommendations on future research are presented.

7.1 Conclusions

The studies presented in this thesis aim to investigate Safe Operating Envelopes (SOE) of heavy vehicle combinations and utilize such envelopes in real-time control to sustain stability in control allocation. First, yaw instability modes of vehicle combinations are explained. Then an SOE that limits the braking and propulsion forces of the combination as a function of lateral acceleration is introduced. Such SOEs can be obtained with either single-track (**Paper A**) or two-track (**Paper C**) models with varying complexities for the tire models, or with a high-fidelity simulation model (**Paper B**). It is possible to generate SOEs via a two-track vehicle model with a combined slip tire model with high accuracy. Furthermore, since this model can accurately estimate the limiting conditions for stable and unstable maneuvers, it can be used in model-based control methods, such as model predictive control, to allocate the forces into different units in a stable way.

The SOE obtained with a high-fidelity model is validated with real vehicle tests. Furthermore, the effects of different environmental parameters (such as friction and slope), and vehicle states (such as load distribution or speed) on the SOE are investigated. It is shown that SOEs would expand or shrink for different parameters, hence it is important to store the related SOEs for the instantaneous operating conditions.

In **Paper D**, the envisioned hierarchical control allocation functional architecture is introduced. Control allocation is performed in two layers: the upper-level handles the combination control allocation, and the lower-level handles the unit control allocation. Then real-time control allocation of a tractor-semitrailer combination is performed during brake-in-turn maneuvers on slippery road surfaces. Control allocation is achieved via power loss minimization. Without additional safety algorithms, jackknifing occurs due to extensive braking with the electric axles of the tractor while only focusing on power loss minimization. When an SOE is used as inequality constraints together with the minimization algorithm, braking is safely performed with no jackknifing. By this, it is demonstrated that integration of an SOE to the control allocation problem results in safer driving.

Furthermore, three other methods to ensure yaw stability while solving a control allocation problem are demonstrated. The first is estimating the lateral tire forces and limiting the Electric Motor (EM) force capabilities according to a friction circle. The second is measuring the lateral acceleration and longitudinal wheel slips, and when these quantities grow beyond a limit, detecting a yaw instability and limiting the EM forces. The third is measuring the lateral acceleration and side-slip angles of the units, and limiting the EM forces when a yaw instability is detected. All these methods ensure a safe control allocation already at the combination level.

Using SOE and limiting the longitudinal force capabilities based on the estimated lateral tire forces are proactive methods aiming to prevent any yaw instability before it starts to happen. Furthermore, they utilize a model-based approach since for generating SOE, and for estimating the lateral tire forces, vehicle models are used. This requires knowledge of the vehicle parameters. Hence, the trailing unit parameters such as wheelbase should be communicated with the towing unit for these methods to perform well. Additionally, these methods require the knowledge of the road friction coefficient, hence a friction estimator is needed. As long as the vehicle and environmental parameters are known, these model-based proactive methods should ensure yaw stability.

Reducing the longitudinal force capabilities when high lateral acceleration and high longitudinal or lateral slip are detected are reactive methods. This means that capabilities are reduced after certain states of the vehicles have reached critical levels. These methods do not require knowledge of the vehicle parameters or the road friction. However, for decreasing the capabilities based on lateral slip, a side-slip angle estimator is needed. If the proactive methods fail to ensure yaw stability, reactive methods can be used to maintain safety as a backup solution.

In **Paper E**, an alternative approach to ensure safe control allocation is presented, utilizing slip limits instead of force limits. In a propel-in-turn maneuver, a reference side-slip angle for the tractor is obtained via an estimator, and the longitudinal slip limit of the EMs is reduced for any deviation from the reference side-slip angle. Following the simulations, the developed control method is tested in real vehicle tests, and shown that it improves yaw stability, traction, and acceleration time compared to fixed slip limits.

Proactive and model-based methods such as the SOE and limiting the force capabilities with respect to a friction circle rely on knowledge of the friction coefficient and some other vehicle states. These can be obtained from a motion estimator and used for ensuring a safe control allocation. If the friction, lateral tire force estimation, and other required quantities are uncertain or difficult to estimate, SOE and friction circle limitation can be implemented by using a relaxed set of constraints meaning that they may not ensure a safe allocation in challenging cases like low friction surfaces. In such cases, reactive methods (such as reducing EM capabilities when lateral or longitudinal slips increase significantly) can be used as a safety net. Even though they cannot fully ensure that a yaw instability will not happen, once an instability starts they would timely intervene and save the vehicles from a catastrophic accident. Additionally, adaptive longitudinal slip limits can be used together with the force-based methods, contributing to both safe and efficient driving.

7.2 Future outlook

The safe operating envelope in the force domain is extensively studied in the papers presented in this research. Safety limits in the slip domain are also investigated, and a method for estimating a reference side-slip angle and decreasing the longitudinal slip limit for the deviations from the reference side-slip angle is simulated and tested with real vehicles. However, slip limits should be studied in detail. It is expected that the size of the safe side-slip margin would depend on friction. For higher frictions, tires would be able to generate higher lateral forces with higher side-slip angles compared to lower frictions. Therefore, the effect of friction on the safe operating envelope should be studied as a natural extension of the studies presented so far. Furthermore, alternative safe envelopes in different states can be formulated, such as side-slip angle versus yaw rate, or lateral velocity versus yaw rate. Phase plane trajectories of such states should be derived and considered during control allocation.

In this study, only the safety aspect of control allocation is studied. Particularly, divergent yaw instabilities like jackknifing and trailer swing are investigated. As a future work, dynamic yaw instabilities like trailer sway, and roll stability should be studied.

After the detailed investigation of the safety aspect of the control allocation at the combination level presented in this thesis, it is aimed to focus on the energy-efficiency aspect. Power loss minimization in a heavy vehicle combination with multiple electrified units will be studied. Particularly, power loss minimization with a centralized control allocator will be compared to a control allocator with a hierarchical algorithmic structure.

Bibliography

[1] I. Katsarova, "Weights and dimensions of road vehicles in the EU," European Parliamentary Research Service, 2014. Accessed: Apr. 29, 2024. [Online]. Available: europarl.europa.eu/RegData/bibliotheque/briefing/2014/140796/LDM_BRI%282014%29140796_REV1_EN.pdf

[2] S. Kharrazi, L. Laine, L. Larsson, J. Sandin, B. Jacobson, T. Asp, and O. Bagdadi. (Nov. 2023). A review of more than a decade of research and field tests on longer vehicle combinations in Sweden that supported road approval. Presented at 17th Int. Symp. on Heavy Vehicle Transp. & Technol. (HVTT17), Brisbane, Australia. [Online]. Available: hvttforum.org/wp-content/uploads/2024/02/HVTT17_paper_7891_Kharrazi.pdf

[3] European Parliament News. "Parliament to decide on longer and heavier "green" trucks." europarl.europa.eu. Accessed: Apr. 29, 2024. [Online]. Available: europarl.europa.eu/news/en/agenda/briefing/2024-03-11/18/parliament-to-decide-on-longer-and-heavier-green-trucks

[4] ZF. "ZF´s Electrified Trailer Solution." zf.com. Accessed: Apr. 29, 2024. [Online]. Available: zf.com/products/en/cv/stories_content_pages/electrified_trailer_solution.html

[5] Trailer Dynamics. "eTrailer." trailerdynamics.de. Accessed: Apr. 29, 2024. [Online]. Available: trailerdynamics.de/en/etrailer/

[6] Einride. "Einride Trailer." einride.tech. Accessed: Apr. 29, 2024. [Online]. Available: einride.tech/electric/trailer

[7] Schmitz Cargobull. "Schmitz Cargobull electric reefer semi-trailer with e-axle secures type approval." cargobull.com. Accessed: Apr. 29, 2024. [Online]. Available: cargobull.com/en/press/2023/typgenehmigung_skoe_cool

[8] N. Bradford. "How Octopus Arms Bypass the Brain." scientificamerican.com. Accessed: Apr. 29, 2024. [Online]. Available: scientificamerican.com/article/how-octopus-arms-bypass-the-brain/

[9] G. Levy, T. Flash, and B. Hochner, "Arm coordination in octopus crawling involves unique motor control strategies," *Current Biology*, vol. 25, no. 9, pp. 1195-1200, May 2015, doi: 10.1016/j.cub.2015.02.064.

[10] G. Barathieu. "UPY 2017 Award Winners - Underwater Photographer of the Year." underwaterphotographeroftheyear.com. Accessed: Apr. 29, 2024. [Online]. Available: underwaterphotographeroftheyear.com/archive/2017-winning-images/award-winners/1/

[11] Volvo Trucks. Volvo Trucks - Volvo Trucks vs 750 Tonnes: An extreme heavy haulage challenge. (Apr. 12, 2016). Accessed: Apr. 29, 2024. [Online Video]. Available: youtube.com/watch?v=5UUz1zTZFfU&ab_channel=VolvoTrucks

[12] Volvo Trucks. "Volvo FH Electric." volvotrucks.com. Accessed: Apr. 29, 2024. [Online]. Available: volvotrucks.com/en-en/trucks/electric/volvo-fh-electric.html

[13] L. Laine, "Reconfigurable motion control systems for over-actuated road vehicles," Ph.D. dissertation, Dept. Appl. Mechanics, Chalmers Univ. of Technol., Gothenburg, Sweden, 2007. [Online]. Available: research.chalmers.se/en/publication/41492

[14] M. Gäfvert, "Topics in modeling, control, and implementation in automotive systems," Ph.D. dissertation, Dept. Autom. Control, Lund Inst. of Technol., Lund, Sweden, 2003. [Online]. Available: portal.research.lu.se/files/4840790/8571803.pdf

[15] T. Ghandriz, "Transportation mission-based optimization of heavy combination road vehicles and distributed propulsion, including predictive energy and motion control," Ph.D. dissertation, Dept. Mechanics and Maritime Sci., Chalmers Univ. of Technol., Gothenburg, Sweden, 2020. [Online]. Available: research.chalmers.se/en/publication/?id=520358

[16] J. Torinsson, "Power loss minimization in electric cars by wheel force allocation," Lic. thesis, Dept. Mechanics and Maritime Sci., Chalmers Univ. of Technol., Gothenburg, Sweden, 2020. [Online]. Available: research.chalmers.se/en/publication/520503

[17] T. Ghandriz, "Transportation mission-based optimization of heavy combination road vehicles and distributed propulsion, including predictive energy and motion control," Ph.D. dissertation, Dept. Mechanics and Maritime Sci., Chalmers Univ. of Technol., Gothenburg, Sweden, 2020. [Online]. Available: research.chalmers.se/en/publication/?id=520358

[18] O. Härkegård, ”Backstepping and control allocation with applications to flight control,” Ph.D. dissertation, Dept. Elect. Eng., Linköping Univ., Linköping, Sweden, 2003. [Online]. Available: diva-portal.org/smash/get/diva2:243491/FULLTEXT01.pdf

[19] J. Torinsson, M. Jonasson, D. Yang, and B. Jacobson, ”Energy reduction by power loss minimisation through wheel torque allocation in electric vehicles: a simulation-based approach,” *Vehicle System Dyn.*, vol. 60, no. 5, pp. 1488-1511, 2022, doi: 10.1080/00423114.2020.1858121.

[20] S. Janardhanan, L. Laine, M. Jonasson, B. Jacobson, and E. Gelso, ”Motion control and power coordination of electric propulsion and braking distributed on multiple axles on heavy vehicles,” in *2022 IEEE Vehicle Power and Propulsion Conf. (VPPC)*, Merced, CA, USA, Nov. 2022, pp. 1-8, doi: 10.1109/VPPC55846.2022.10003450.

[21] ISO. ”ISO 11992-4:2023.” iso.org. Accessed: Apr. 29, 2024. [Online]. Available: iso.org/standard/79622.html

[22] J. Aurell and C. B. Winkler. (1995). Standard test procedures for the lateral stability of heavy vehicle combinations. Presented at 4th Int. Symp. on Heavy Vehicle Weights and Dimensions. & Technol. (HVWD4), Ann Arbor, MI, USA. [Online]. Available: hvttforum.org/wp-content/uploads/2019/11/Standard-Test-Procedures-For-The-Lateral-Stability-Of-Heavy-Vehicle-Combinations-Aurell-.pdf

[23] Transportstyrelsen, ”TSFS 2018:40 Transportstyrelsens föreskrifter och allmänna råd om tekniska krav på fordonståg med bruttovikt över 64 ton och längd om högst 25,25 meter,” Transportstyrelsen, 2018. Accessed: Apr. 29, 2024. [Online]. Available: transportstyrelsen.se/TSFS/TSFS%202018_40k.pdf

[24] S. Kharrazi, B. Augusto, and N. Fröjd, ”Assessing dynamics of heavy vehicles in a driving simulator,” *Transp. Res. Part F: Traffic Psychol. and Behav.*, vol. 65, pp. 306-315, 2019, doi: 10.1016/j.trf.2019.07.007.

[25] J. Aurell and T. Wadman, ”Vehicle combinations based on the modular concept,” Nordiska Vägtekniska Förbundet, Report no. 1/2007, 2007. Accessed: Apr. 29, 2024. [Online]. Available: nvfnorden.org/wp-content/uploads/2020/10/2007-Vehicle-combinations-based-on-the-modular-concept-Background-and-analysis.pdf

[26] Toyota. ”Hilux How To: Trailer Sway Control .” toyota.co.uk. Accessed: Apr. 29, 2024. [Online]. Available: mag.toyota.co.uk/hilux-trailer-sway-control/

[27] Bosch. "Trailer safety control." bosch-mobility.com. Accessed: Apr. 29, 2024. [Online]. Available: bosch-mobility.com/en/solutions/driving-safety/trailer-safety-control/

[28] AL-KO. "ATC: AL-KO Trailer Control." alko-tech.com. Accessed: Apr. 29, 2024. [Online]. Available: alko-tech.com/en/Vehicle-types-products/atc-al-ko-trailer-control_pdt_227

[29] Q. Wang and Y. He, "A study on single lane-change manoeuvres for determining rearward amplification of multi-trailer articulated heavy vehicles with active trailer steering systems," *Vehicle System Dyn.*, vol. 54, no. 1, pp. 102–123, 2016, doi: 10.1080/00423114.2015.1123280.

[30] Volvo Trucks. "Full-scale crash tests of Volvo's electric trucks." volvotrucks.com. Accessed: Apr. 29, 2024. [Online]. Available: volvotrucks.com/en-en/news-stories/stories/2022/dec/full-scale-crash-tests-of-volvo-s-electric-trucks.html

[31] Volkswagen. "Active roll stabilization." volkswagen-newsroom.com. Accessed: Apr. 29, 2024. [Online]. Available: volkswagen-newsroom.com/en/active-roll-stabilization-3944

[32] B. Chen and H. Peng, "Differential-braking-based rollover prevention for sport utility vehicles with human-in-the-loop evaluations," *Vehicle System Dyn.*, vol. 36, no. 4-5, pp. 359-389, 2001, doi: 10.1076/vesd.36.4.359.3546.

[33] V. F. Dal Poggetto and A. L. Serpa, "Vehicle rollover avoidance by application of gain-scheduled LQR controllers using state observers," *Vehicle System Dyn.*, vol. 54, no. 2, pp. 191-209, 2016, doi: 10.1080/00423114.2015.1125005.

[34] B. Jacobson, "Combined longitudinal and lateral Slip," in *Vehicle Dyn. Compendium*. Gothenburg, Sweden: Chalmers University of Technology, 2020, ch. 2, sec. 2.5, pp 133-134. [Online]. Available: research.chalmers.se/publication/520229/file/520229_Fulltext.pdf

[35] N. Fröjd. "Handling analysis and control development of commercial trucks with Volvo transport models." mathworks.com. Accessed: Apr. 29, 2024. [Online]. Available: se.mathworks.com/videos/handling-analysis-and-control-development-of-commercial-trucks-with-volvo-transport-models-1622035211192.html

[36] R. Fu, H. Zhang, Y. Guo, F. Yang, and Y. Lu, "Real-time estimation and prediction of lateral stability of coaches: a hybrid approach based on EKF, BPNN, and online autoregressive integrated moving average algorithm," *IET*

Intell. Transp. Syst., vol. 14, no. 13, pp. 1892-1902, 2020, doi: 10.1049/iet-its.2020.0385.

[37] J. Funke, M. Brown, S. M. Erlien, and J. C. Gerdes, "Collision avoidance and stabilization for autonomous vehicles in emergency scenarios," *IEEE Trans. Control Syst. Technol.*, vol. 25, no. 4, pp. 1204-1216, July 2017, doi: 10.1109/TCST.2016.2599783.

[38] S. M. Erlien, S. Fujita, and J. C. Gerdes, "Shared steering control using safe envelopes for obstacle avoidance and vehicle stability," *IEEE Trans. Intell. Transp. Syst.*, vol. 17, no. 2, pp. 441-451, Feb. 2016, doi: 10.1109/TITS.2015.2453404.

[39] B. Jacobson, "Anisotropic brush model with independent bristles," in *Vehicle Dyn. Compendium.* Gothenburg, Sweden: Chalmers University of Technology, 2020, ch. 2, sec. 2.5.1, pp 134-137. [Online]. Available: research.chalmers.se/publication/520229/file/520229_Fulltext.pdf

[40] Colmis AB. "Test Tracks." colmis.com. Accessed: Jan. 24, 2024. [Online]. Available: colmis.com/test-tracks/